NASA TECHNICAL NOTE

NASA TN D-3400

NASA TN D-3400

A METHOD OF APPROXIMATING PROPELLANT REQUIREMENTS OF LOW-THRUST TRAJECTORIES

by Charles L. Zola

Lewis Research Center
Cleveland, Ohio

NATIONAL AERONAUTICS AND SPACE ADMINISTRATION • WASHINGTON, D. C. • APRIL 1966

A METHOD OF APPROXIMATING PROPELLANT REQUIREMENTS OF LOW-THRUST TRAJECTORIES

By Charles L. Zola

Lewis Research Center
Cleveland, Ohio

NATIONAL AERONAUTICS AND SPACE ADMINISTRATION

For sale by the Clearinghouse for Federal Scientific and Technical Information
Springfield, Virginia 22151 – Price $0.80

CONTENTS

	Page
SUMMARY	1
INTRODUCTION	1
ANALYSIS	3
Constant Thrust Operation	4
Characteristics of Constant Thrust Trajectory Solutions in a Gravity Field	5
Rectilinear Problem Model	7
Rectilinear Problem Solutions	7
Impulsive solution	8
Constant thrust solution	8
All-propulsion case	12
Typical Characteristics of Rectilinear Trajectory Solutions	13
RESULTS AND DISCUSSION	14
Equivalent Rest-to-Rest Length of Actual Solutions	14
Effect of Error in Equivalent Length	16
Sources of Equivalent Length for Trajectory Problems	17
Examples	19
Extended Problem Model	22
CONCLUSION	25
APPENDIXES	
A - SYMBOLS	26
B - RECTILINEAR REST-TO-REST SOLUTIONS	27
C - GENERALIZED CONSTANT THRUST ROCKET PERFORMANCE	30
D - EQUIVALENT LENGTH OF SOME SELECTED TRAJECTORY PROBLEMS	36
REFERENCES	37

A METHOD OF APPROXIMATING PROPELLANT REQUIREMENTS OF LOW-THRUST TRAJECTORIES

by Charles L. Zola

Lewis Research Center

SUMMARY

The precise calculation of optimum trajectory solutions for low-acceleration flight in the inverse-square gravity field can be very complicated and time consuming, particularly in the case of operating with constant thrust and jet velocity. An approximation method is presented that greatly reduces this computation effort. This method is based on the dynamic similarity between flight on an optimum trajectory in the inverse-square field and rest-to-rest flight on a rectilinear path in gravity-free space. Consequently, the equivalent rectilinear path length L becomes a measure of the propulsive effort of trajectories similar to the characteristic velocity increment ΔV. Examples of the use and validity of the method are given for different types of interplanetary trajectory problems.

When applied to typical circular orbit transfer problems, the approximation method can predict ΔV with an error of 10 percent or less. It is shown that errors in the method are most serious for flyby trajectories, becoming as large as 40 percent in terms of ΔV. However, typical specific impulse values for low-acceleration flight reduce the ΔV error by a factor of two or more when translated into error in propellant consumption. The possibility of improving accuracy is discussed, and it is shown that a more general (and more complicated) type of rectilinear flight with nonzero velocities at the terminals may be required.

INTRODUCTION

Accurate trajectory calculations for vehicles with low thrust operating in an inverse-square gravitational field encounter one or both of two major complications. First, the equations of motion cannot, in general, be solved in closed form. Numerical integration procedures must be used to calculate the path in a stepwise fashion. The second major

difficulty stems from the need to control the available thrust acceleration vector over long propulsion times in such a way that the vehicle accomplishes a transfer from one particular position and velocity state to another in a specified time. This transfer problem is called the "point-to-point" problem in this report.

Valid, but nonoptimum solutions of point-to-point problems have been made with arbitrary thrust vectoring policies. For example, the equations of motion presented in reference 1, for thrusting with an arbitrary steering policy, can be employed in the solution of point-to-point problems, but still require numerical integration. In reference 2, both the numerical integration and point-to-point problem difficulties were simplified by closed form solutions made possible by arbitrarily selecting a trajectory path in space and finding an acceleration control history that would satisfy it.

However, many authors (e. g., refs. 3 to 5) have analyzed trajectory problems by applying the calculus of variations or other optimization theory and have shown that nonoptimum thrust vectoring can result in excessive propellant requirements. Therefore, the inclusion of suitable optimization theory has become a highly preferred extension of low-thrust trajectory solution methods and has received much attention.

The main feature of the so-called "optimum" trajectory solution is a program or policy for physical control of the magnitude and/or direction of the available thrust, subject to specified constraints on the operation of the rocket. The result is a different problem formulation for each "mode" or type of rocket operation. Each formulation then provides minimum propellant solutions of point-to-point trajectory problems.

Appropriate constraints can be set up to describe any one of the various modes of rocket operation that are of interest in the calculation of optimum trajectory solutions. One particular mode that is mentioned frequently in this report employs constant jet power with constant thrust and jet velocity and optimized coasting periods (ref. 5). For brevity, in the remainder of this report this mode will be called "constant thrust" operation.

The application of optimization theory improves rocket performance but often adds to the already present computation difficulties. The optimum point-to-point trajectory problem is a two-point boundary value problem, since certain problem variables have values specified at both ends of the trajectory but the complete and correct set of boundary values is not known.

Methods of solving two-point boundary value problems are involved and occasionally unsuccessful. Such problems are often solved as iterated initial value problems. In this procedure the unknown problem variables are estimated at the initial point so that numerical integration of the path may proceed. To find the correct solution of the problem, the unknown initial values are methodically re-estimated, utilizing highly involved iteration schemes, until the specified end conditions are met.

In particular, the constant thrust mode presents one of the most unmanageable prob-

lems in the calculation of optimum trajectories. Yet, this mode of operation is especially interesting because the constant thrust type of ion engine has already been successfully operated and is representative of first generation ion-electric propulsion.

The purpose of this report is to present a rapid approximation technique for optimum trajectory solutions that avoids the computational difficulties mentioned previously. The approximate method given here is applicable to all modes of operation but is particularly aimed at reducing the burden of trajectory calculations for the constant thrust rocket vehicle.

In a previous publication (ref. 6) a brief discussion of this approximation method was given along with examples of its application to Earth-Mars trajectory analysis. This report extends that previous study by presenting a more general analysis and by giving examples of the approximation used for trajectories to other planets. The extent of the validity of the method will also be explored to indicate the magnitude and effect of errors. A generalized, dimensionless trajectory analysis procedure based on the approximate method is outlined in appendix C.

ANALYSIS

The principal idea in the method of this report is to assume that any given point-to-point trajectory problem in the inverse-square gravity field can be transformed into an equivalent, or corollary, rest-to-rest rectilinear problem in field free space. This equivalent rectilinear trajectory problem can then be easily solved to obtain propellant requirements for any type of rocket operation. Other authors have used simple rectilinear flight to exhibit the differences in rocket performance when the mode of rocket operation is changed (refs. 7 and 4). In this report, similar expressions are also used; but, in addition, an approximation scheme for optimum trajectory solutions is derived by noting the dynamic similarity between rectilinear, gravity-free flight and optimum flight in the inverse-square gravity field.

For any type of rocket operation, the propulsive requirement of a rest-to-rest rectilinear trajectory is primarily dependent on the transfer time T and the straight line length travelled L. (Symbols are defined in appendix A.) The travel length of the equivalent rectilinear problem can only be defined, however, by first obtaining an optimum solution of the actual, inverse-square field trajectory problem, using some mode of rocket operation. The actual solution can then be used to convert the trajectory problem into an equivalent straight line problem in field-free space. Further solutions of the original inverse-square field problem are not required. Instead, propellant requirements brought about by any change in rocket operation are obtained by solving its rectilinear counterpart.

Therefore, one reference solution may be calculated using a mode of rocket operation that is more convenient from the standpoint of computation effort. For example, It will be shown that the familiar high-thrust or "impulsive" trajectory method can be used as a reference solution. Also discussed is the use of a low-thrust type of trajectory solution which appears to present a minimum of computation difficulties. This is the constant jet power, variable thrust method of references 3 and 4.

To apply the approximate method of this report, analytic solutions of the rectilinear flight in gravity-free space must be made for various modes of rocket operation.

A development of some of these analytical solutions will be made in this analysis. But first a preliminary discussion of the parameters and characteristics of inverse-square field, optimum trajectory solutions with constant thrust operation will be presented. At the end of this analysis, similarities between the rectilinear problem model and actual trajectory solutions will be described.

Constant Thrust Operation

The constant thrust mode of rocket operation is characterized by alternate periods of propulsion (thrust on) and coasting (thrust off). During propulsion, it is specified that the thrust F and mass flow rate $\dot{m}$ are constant. During coasting periods, F and $\dot{m}$ are zero. In this report, the initial acceleration a_o is often used, where

$$a_o \equiv \frac{F}{m_o} \tag{1}$$

and m_o is the initial mass of the rocket vehicle. Also, the effective jet velocity of the expelled mass v_j will be used in place of $\dot{m}$, with the definition that

$$v_j \equiv \frac{F}{|\dot{m}|} \tag{2}$$

Often, instead of v_j, the specific impulse I will be used as an index of jet velocity with the definition that I is the ratio of F and the weight flow rate (in Earth-surface units)

$$I \equiv \frac{F}{\dot{w}} = \frac{F}{\dot{m}g} = \frac{v_j}{g} \tag{3}$$

Thus I and v_j are simply related through g, the standard acceleration of gravity on the surface of the Earth. When definitions (1) and (2) are used, the mass m and acceleration a at any point on the trajectory are functions of a_o, v_j, and the instantaneous value of accumulated propulsion time t_a; that is,

$$m = m_o - \frac{Ft_a}{v_j} = m_o \left(1 - \frac{a_o t_a}{v_j}\right) \tag{4}$$

$$a = \frac{F}{m} = \frac{F}{m_o \left(1 - \frac{a_o t_a}{v_j}\right)} = \frac{a_o}{1 - \frac{a_o t_a}{v_j}} \tag{5}$$

The accumulation of propulsion time may be interrupted by coasting periods ($F = \dot{m} = 0$) during which t_a does not increase.

Characteristics of Constant Thrust Trajectory Solutions in a Gravity Field

Different values of a_o and v_j can be used in the solution of a given trajectory problem. Each applied combination of a_o and v_j would give rise to different values of required total propulsion time and propellant consumption. When v_j is made infinite, equations (4) and (5) show that mass and acceleration are constant. This infinite v_j case is called the constant acceleration mode (although coast periods with $a = 0$ may be present). The "impulsive" type of trajectory solution may also be included in the general family of solutions with constant thrust rocket operation as cases where F and, therefore, a are infinite.

Typical characteristics of a full range of constant thrust solutions of a given trajectory problem in the inverse-square gravity field are shown in sketch (a). This sketch is a plot of the equivalent total characteristic velocity increment or ΔV of constant thrust solutions as a_o and v_j (or I) are given different values ranging all the way to infinity while the point-to-point trajectory problem is kept unchanged. The ΔV plotted in sketch (a) is derived by taking the integral of the acceleration magnitude history used in each solution of the given problem. For the constant thrust mode of

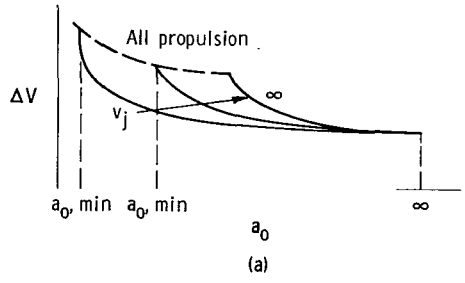

(a)

operation, equation (5) may be integrated to give ΔV as a function of a_o, v_j, and t_p; that is,

$$\Delta V = \int_0^{t_p} |a| \, dt = -v_j \ln \left(1 - \frac{a_o t_p}{v_j}\right) \tag{6}$$

where t_p is the total propulsion time used in the trajectory solution. For constant acceleration solutions ($I = v_j = \infty$), a is constant and equation (6) reduces to

$$\Delta V = a t_p$$

It should be noted that the ΔV for $a_o = \infty$ is the same ΔV commonly used in infinite thrust (impulsive) trajectory analysis as an indication of propellant consumption where

$$\frac{m_p}{m_o} = 1 - e^{-\Delta V / I_g}$$

The characteristics shown in sketch (a) apply, in general, to all optimum, constant thrust solutions of a trajectory problem in the inverse-square gravitational field. It will be shown that solutions of rectilinear trajectory problems in gravity-free space exhibit the same behavior. The most pertinent aspects are the following:

(1) Total ΔV is bounded. The minimum value of ΔV occurs at the impulsive solution ($a = \infty$) regardless of v_j. The upper bound on ΔV consists of solutions classified as "all propulsion". All-propulsion solutions have no coasting periods and represent the lowest value of a_o that may be used for each v_j. The range of ΔV between these bounds applies to operation with finite values of a_o on trajectories that have both propulsion and coasting.

(2) Both a_o and v_j have an effect on ΔV. When a_o is fixed, ΔV increases with increasing v_j, reaching an upper limit at either the all-propulsion value or the constant acceleration coasting case ($v_j = \infty$). Along the all-propulsion boundary, ΔV decreases with increasing v_j, minimizing at the all-propulsion constant acceleration case when $v_j = \infty$. When a_o is greater than the a_o of the all-propulsion constant acceleration case, trajectory solutions will have a coast phase regardless of the value of v_j.

Thus, the presence of the two parameters, a_o and v_j, calls for repeated optimum solutions of the same trajectory problem in order that the range of possible ΔV values be accurately determined. To avoid this extra computation effort, the approximate method of this report is capable of predicting the ΔV at any a_o and v_j provided that

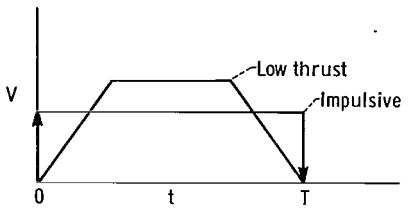

(b)

one optimum solution of the trajectory problem is available for use as a reference in defining L of the equivalent rectilinear trajectory problem.

Rectilinear Problem Model

The approximate trajectory method given in reference 6 was based on the assumption that rest-to-rest rectilinear flight in field-free space provided an adequate problem model for analyzing the performance of constant thrust rockets. It was pointed out that rest-to-rest rectilinear trajectory solutions possess the characteristics described in sketch (a). Sketch (b) is given to show the typical time-history of velocity along the trajectory of a rest-to-rest rectilinear problem. The impulsive type of trajectory solution is shown by the rectangular curve in sketch (b). An instantaneous change in velocity is given at time zero and time T. The two velocity increments are equal because the trajectory problem is to begin at rest (V = 0) and end at rest. The distance covered is the area under the rectangle and is, therefore, proportional to the amount of velocity increment provided at time zero. Also, since there are no losses in this problem model, total ΔV is simply equal to the sum of the two equal velocity increments.

A typical low-thrust case is also shown (trapezoidal curve) in sketch (b). The low-thrust case has two propulsion periods, with equal velocity changes occurring in each. The constant velocity period is a coast during which the acceleration is zero. The distance covered is the sum of the areas under the increasing, constant, and decreasing velocity phases. It can be seen in sketch (b) that, if the distance to be traversed is the same for the low- and high-thrust cases, the ΔV requirement of the low-thrust case will always be greater than the impulsive ΔV.

Other problem models may be used, but the primary aim is to avoid complexity. Later, in the section RESULTS AND DISCUSSION, it will become clear that, in some cases, the rest-to-rest rectilinear problem model is highly inadequate. The possible reason for this is discussed.

Rectilinear Problem Solutions

The subsequent sections of this analysis will consist of developing solutions of the gravity-free, rest-to-rest rectilinear problem. The two cases described here are for the impulsive and constant thrust solutions of the rectilinear trajectory problem. Other solutions of the rest-to-rest rectilinear problem for the constant acceleration and power-limited variable thrust rocket operation modes are given in appendix B.

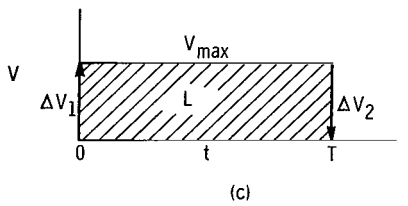

(c)

Impulsive solution. - Sketch (c) shows the velocity history of an impulsive solution of the rectilinear problem model. The first velocity increment ΔV_1 changes the velocity from zero to V_{max}, which is the value required to bring the vehicle to the distance L at time T. The rocket proceeds at constant velocity until time T when it is brought back to rest (zero velocity) instantly by applying a second increment ΔV_2. The distance covered or characteristic length L is the area under the velocity curve.

$$L = V_{max} T = \Delta V_1 T$$

The total required velocity increment ΔV is the sum of the two equal increments ΔV_1 and ΔV_2. Therefore, L can be expressed as a function of total ΔV and T; that is,

$$L = \Delta V_1 T = \frac{\Delta V T}{2} \tag{7}$$

Equation (7) can be interpreted as showing that the total ΔV and transfer time of an impulsive trajectory solution infer a length of travel.

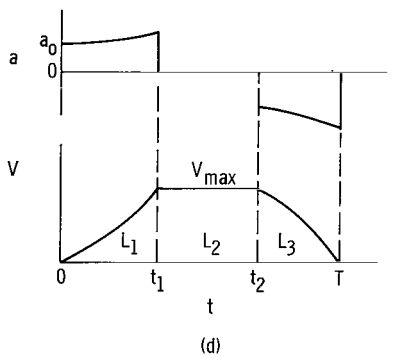

(d)

Constant thrust solution. - Sketch (d) depicts a rest-to-rest rectilinear flight for a constant thrust rocket. This case is not as simple and straightforward as the impulsive thrust case. The magnitude of the acceleration increases during the initial propulsion phase (between 0 and t_1) according to equation (5). The acceleration is zero during the coast phase (between t_1 and t_2). At t_2 the acceleration resumes at the same magnitude it had at t_1 continuing to increase as propellant is consumed in the final propulsion phase. This acceleration history gives rise to the accompanying velocity history. The velocity builds up from zero to V_{max} during the first propulsion phase, remains constant during the coast, then is brought back to zero during the final propulsion phase.

From the velocity history in sketch (d), it is evident that the total length traveled L is the sum of the lengths covered in the initial propulsion phase, the coast, and the final propulsion phase; that is,

$$L = L_1 + L_2 + L_3$$

and

$$L = \int_0^{t_1} V\,dt + \int_{t_1}^{t_2} V\,dt + \int_{t_2}^{T} V\,dt$$

In the initial propulsion phase, the velocity history is a function of the acceleration history. Thus,

$$V = \int_0^t \frac{a_o}{1 - \frac{a_o t}{v_j}}\,dt = -v_j \ln\left(1 - \frac{a_o t}{v_j}\right) \tag{8}$$

and, for $t = t_1$ the velocity has reached a value noted as V_{max}, the coast velocity, in sketch (d); that is,

$$V = V_{max} = -v_j \ln\left(1 - \frac{a_o t_1}{v_j}\right) \tag{9}$$

The length travelled in the first phase L_1 is the integral of the velocity history from 0 to t_1 or

$$L_1 = \int_0^{t_1} V\,dt = \int_0^{t_1} -v_j \ln\left(1 - \frac{a_o t}{v_j}\right)dt$$

and

$$L_1 = \frac{v_j^2}{a_o}\left[\left(1 - \frac{a_o t_1}{v_j}\right)\ln\left(1 - \frac{a_o t_1}{v_j}\right) + \frac{a_o t_1}{v_j}\right] \tag{10}$$

In the coast phase, the rocket covers the distance L_2, which is simply the product of the coast velocity and the duration of coast; that is,

$$L_2 = V_{max}(t_2 - t_1)$$

and

$$L_2 = -(t_2 - t_1)v_j \ln\left(1 - \frac{a_o t_1}{v_j}\right) \tag{11}$$

No mass is consumed in the coast phase; therefore, the acceleration magnitude at t_2 is the same as at t_1. In the third phase, the acceleration history is

$$a = \frac{a_o}{1 - \frac{a_o t_1}{v_j} - \frac{a_o(t - t_2)}{v_j}} \qquad t_2 \leq t \leq T$$

As seen in sketch (d), this acceleration is directed opposite to that of the first phase to decrease the velocity and bring the vehicle to rest at T.

With the same approach used in developing equation (10) for the first phase and the added fact that the velocity change in the third phase is equal to the velocity increment in the first phase, it can be shown that the length increment of the third phase is related to the length increment of the first. The resultant equation for L_3 is

$$L_3 = \frac{v_j^2}{a_o}\left[\left(\frac{a_o t_1}{v_j}\right)^2 - \left(1 - \frac{a_o t_1}{v_j}\right)\ln\left(1 - \frac{a_o t_1}{v_j}\right) - \frac{a_o t_1}{v_j}\right]$$

or using equation (10) results in

$$L_3 = a_o t_1^2 - L_1 \tag{12}$$

The total length L can then be written as the sum of lengths L_1, L_2, and L_3

$$L = a_o t_1^2 - (t_2 - t_1)v_j \ln\left(1 - \frac{a_o t_1}{v_j}\right) \tag{13}$$

A more useful form of equation (13) may be expressed in terms of the total time T and the total propulsion time t_p of the transit. In sketch (d), the total velocity increment that must be provided by the rocket is $2V_{max}$, because the rocket undergoes a

change of V_{max} in the first phase and another change of V_{max} in the third phase. From equation (6), for a rocket in the constant thrust mode

$$\Delta V = -v_j \ln \left(1 - \frac{a_o t_p}{v_j}\right)$$

Therefore, V_{max} can be related to t_p

$$V_{max} = \frac{\Delta V}{2} = -\frac{v_j}{2} \ln \left(1 - \frac{a_o t_p}{v_j}\right) \tag{14}$$

But, from equation (9)

$$V_{max} = -v_j \ln \left(1 - \frac{a_o t_1}{v_j}\right)$$

Therefore, if equations (9) and (14) are combined, t_1 is related to t_p

$$\ln \left(1 - \frac{a_o t_1}{v_j}\right) = \frac{1}{2} \ln \left(1 - \frac{a_o t_p}{v_j}\right) \tag{15}$$

which leads to

$$a_o t_1^2 = \frac{v_j^2}{a_o} \left(1 - \sqrt{1 - \frac{a_o t_p}{v_j}}\right)^2 \tag{16}$$

Also, since $t_2 - t_1$ is the coast time, it can be expressed as a function of T and t_p

$$t_2 - t_1 = T - t_p \tag{17}$$

Substitution of equations (15), (16), and (17) into the length relation (eq. (13)) results in

$$L = \frac{v_j^2}{a_o} \left(1 - \sqrt{1 - \frac{a_o t_p}{v_j}}\right)^2 - \frac{(T - t_p)}{2} v_j \ln \left(1 - \frac{a_o t_p}{v_j}\right) \tag{18}$$

Equation (18) gives the length of travel for a constant thrust rocket, with coasting, on a straight line path in field-free space. The first term of equation (18) is the length covered in the propulsion phases. The second term is the length covered in the coast phase. It is simply a product of the coast time $(T - t_p)$ and the coast velocity $\left[-\frac{v_j}{2} \ln \left(1 - \frac{a_o t_p}{v_j}\right)\right]$. If a_o is allowed to pass to infinity, t_p will become zero. In this limiting case, equation (18) reduces to the impulsive case (eq. (7)), illustrating that the impulsive case is simply a special form of constant thrust with coasting. In fact, impulsive thrust might be termed an "all-coasting" solution.

Equation (7), for impulsive thrust, provides a simple relation between the impulsive ΔV requirement and L. Similarily, equations (6) and (18) can be combined to give an expression for the ΔV requirement of the constant thrust mode of operation; that is,

$$\Delta V = -v_j \ln \left(1 - \frac{a_o t_p}{v_j}\right)$$

and

$$\Delta V = \frac{2a_o L - 2v_j^2 \left(1 - e^{-\Delta V/2v_j}\right)^2}{a_o T - v_j \left(1 - e^{-\Delta V/v_j}\right)} \tag{19}$$

Equation (19) is, however, transcendental in terms of ΔV but can be solved by simple iterative methods.

All-propulsion case. - All-propulsion solutions are another special case of constant thrust trajectories. They are, nevertheless, of much significance in constant thrust solutions because, as pointed out in the discussion of sketch (a) (p. 5), the all-propulsion solution of a given trajectory with a given v_j has the lowest possible value of initial acceleration. This is an important consideration in constant thrust trajectories because it shows that some combinations of a_o and v_j cannot result in a real solution of a given trajectory problem. Rectilinear trajectory solutions with constant thrust have this same characteristic.

In the case of all propulsion, propulsion time is equal to total transfer time. If t_p is set equal to T in equation (18), the result is a length equation for constant thrust, all-propulsion solutions of the rectilinear problem; that is,

$$L = \frac{v_j^2}{a_o}\left(1 - \sqrt{1 - \frac{a_o T}{v_j}}\right)^2 \tag{20}$$

If the length of travel, L, and the time of travel, T, are fixed, equation (20) serves to provide unique relations between the jet velocity and initial acceleration for all-propulsion solutions. For example, equation (20) can be solved for initial acceleration.

$$a_o = \frac{4L}{T^2}\left(\frac{v_j}{v_j + \frac{L}{T}}\right)^2 \tag{21}$$

One useful interpretation of this equation is that, for a given L, T, and v_j, the minimum a_o that may be used for the rectilinear trajectory can be immediately calculated for comparison with some other a_o which may be desired. If the desired a_o is less than the all-propulsion value, a solution is not possible.

In appendix C, equations (18) and (20) are converted to dimensionless parameters involving acceleration, jet velocity, and ΔV. The dimensionless relations prove to be very useful in that they allow the plotting of generalized performance curves for constant thrust mode, rectilinear trajectory solutions.

Typical Characteristics of Rectilinear Trajectory Solutions

Up to this point, equations have been developed that relate L of the rectilinear, rest-to-rest trajectory with a_o, v_j, t_p, and T for the constant thrust rocket with or without coasting. The typical characteristics of a constant thrust, rectilinear, gravity-free trajectory will now be described, using these equations, to point out the basic similarity between solutions of this simple problem and the optimum, constant thrust, inverse-square field solutions described in sketch (a).

If a simple trajectory problem is stated consisting of a given length and travel time, equations (18) and (20) can be used to prepare a ΔV chart, such as figure 1. In figure 1, ΔV is plotted against a_o for a range in v_j. For the coasting solutions in figure 1, equation (18) is used to evaluate the final mass fraction m_f/m_o,

$$\frac{m_f}{m_o} = 1 - \frac{a_o t_p}{v_j}$$

for the given L and T at various values of a_o and v_j. Then equation (6) is used to evaluate ΔV. The line of all-propulsion solutions in figure 1 is constructed with equations (20) and (6).

Although figure 1 os valid only for the stated gravity-free rectilinear problem, the characteristic behavior of the plotted curves is typical of actual inverse-square field constant thrust results outlined in the discussion of sketch (a). Along the all-propulsion boundary curve, ΔV varies with jet velocity, reaching a minimum at infinite jet velocity. The all-propulsion, infinite jet velocity point has the least ΔV and the highest a_o of all the possible all-propulsion solutions of this problem. For the specified L (10^{11} m) and T (10^7 sec), the impulsive or infinite a_o solutions has a ΔV of 2×10^4 meters per second, given by equation (7). This impulsive ΔV is the least possible ΔV and is not affected by v_j as was also true in sketch (a).

RESULTS AND DISCUSSION

The purpose of this section is to present data concerning the accuracy and use of the approximation method by applying the rectilinear problem model to actual optimum trajectory solutions. First, the equivalent length will be evaluated, over a range of values of a_o for optimum, constant thrust mode solutions of several point-to-point trajectory problems. This is to check the validity of the assumption that L evaluated at any acceleration level will be nearly the same, as long as the trajectory problem is fixed. The effect of using optimum variable thrust (ref. 4) solutions of each trajectory problem to evaluate L will also be discussed. Finally, it will be shown that, once a representative value of L for a trajectory problem is found, the simple relations derived in the preceding section may be applied to obtain values of ΔV or propellant consumption as a function of a_o and v_j that are comparable to detailed optimum constant thrust solutions.

Equivalent Rest-to-Rest Length of Actual Solutions

Figure 1, for the rectilinear problem with fixed L and T, suggests the possibility that a given point-to-point trajectory problem in the inverse-square field might be represented as a simple rest-to-rest rectilinear problem in field-free space. The equivalent length of any problem would, ideally, be unaffected by the mode of rocket operation. For example, all possible constant thrust solutions (all propulsion, partial coasting, or all coasting) of a given problem would indicate the same value of L. The validity of this presumption is examined in figures 2 to 6.

Figure 2 is based on optimum constant thrust solutions of three, Earth to Mars, point-to-point, trajectory problems. A range of values of a_o is shown for each case,

from the all-propulsion point (least a_o) to the impulsive solution ($a_o = \infty$). The heliocentric trajectory problems in figure 2 are "capture" cases in that they begin in circular orbit about the Sun at Earth's radius and end in circular orbit about the Sun at Mars' radius at the end of the stated transfer time T and elapsed heliocentric central angle φ. Thus these examples are point-to-point trajectory problems in that position and velocity are completely specified at each boundary. Each solution (at each a_o) was converted into a rectilinear, rest-to-rest problem by using equation (18) and the known values of a_o, v_j, T, and t_p. Figure 3 for a Venus capture and figure 4 for a Jupiter capture were developed in the same manner. Figures 2, 3, and 4 illustrate a small variation in the equivalent L of each trajectory problem as a_o is varied. The curves have a characteristic increase in L as the all-propulsion point is approached. This increased L indicates that the actual ΔV is higher, relative to high a_o solutions, than the rest-to-rest rectilinear model would predict. Figure 4, the Jupiter case, shows that L is also affected some what by the specific impulse used in the reference solution.

In figures 2, 3, and 4 the equivalent L is not constant for each problem, but the error due to using the rest-to-rest problem model would be small since the net change in L for all cases is only about 6 to 10 percent between the impulsive and all-propulsion extremes. For example, in the 200-day Mars capture of figure 2, any one of the optimum solutions, over the range of possible a_o could have been used to evaluate L for this trajectory problem with a maximum expected error of 10 percent. The relation between error in L and error in propellant consumption will be discussed in the section Effect of Error in Equivalent Length.

Figures 5 and 6 are given to show that, apparently for "flyby"-type trajectories, a great deviation in L can occur. Figure 5, the Mars flyby, shows first a decrease, then an increase, in L as the all-propulsion point is approached from infinite a_o. The value of L deviates as much as 12 percent in this case. The shape of the curve in figure 5 simply reflects the difference between actual ΔV for these optimum solutions and the ΔV that would be predicted by the problem model if L were assumed constant through the range at any one of the values shown.

Figure 6, for the solar probe flyby trajectory to 0. 1 astronomical unit, is the worst example given here of the applicability of the problem model to actual trajectory solutions. In this case, the equivalent L varies as much as 42 percent. Such deviations in L are an indication that the rest-to-rest, rectilinear problem model may be insufficient in accurately predicting propulsive requirement of a wide range of trajectory problem types in the inverse-square gravity field. Underlying reasons for such poor correspondence between actual flights and the simple rest-to-rest problem model are discussed in a later section tltled Extended Problem Model.

Effect of Error in Equivalent Length

In the previous section the equivalent lengths of actual solutions of various trajectory problems were calculated and plotted to illustrate that L is not truly invariant when a_o is varied. The worst example of highly variable L were the Mars flyby and the solar probe. The solar probe L varies about 40 percent between the impulsive and all-propulsion solutions. It is obvious in these two flyby examples that the approximate scheme given herein would have extreme inaccuracy. Nevertheless, the solar probe case (fig. 6) will be used to illustrate the effect of errors in L upon propellant requirements.

At any a_o in the constant thrust mode, an error in L produces about the same error in ΔV. For example, from equation (7) for the impulsive case where $\Delta V = 2L/T$, a percentage change in L causes the same percentage change in ΔV. In figure 6 it can be seen that a typical low-acceleration value of L is 10^{11} meters. If this value of L is assumed for the constant thrust cases, the difference between it and the actual L values at each a_o on figure 6 indicates the error in ΔV. In figure 7, the final mass fraction of the actual constant thrust solutions are compared with the approximate results based on $L = 1.0 \times 10^{11}$ meters. The actual constant thrust solutions were calculated using an I = 10 000 seconds; however, another curve at I = 4000 seconds is given to show the growth in error as I is decreased. It can be seen in figure 7 that, even at I = 4000 seconds, the mass fraction errors are not as large as the expected ΔV errors. This error reduction is due to the fact that mass fraction is a function of the ratio $\Delta V/Ig$. Thus,

$$\frac{m_f}{m_o} = r = e^{-\Delta V/Ig}$$

The error in final mass fraction dr/r is a function of the error in ΔV but is modified by the product $\Delta V/Ig$

$$\frac{dr}{r} = \frac{-\Delta V}{Ig} \frac{d\,\Delta V}{\Delta V}$$

Even when I is as low as 4000 in the solar probe case, the term $\Delta V/Ig$ is about 0.5. The result is that the percentage error in r is only half the error in ΔV. This error reduction is due to high values of I and is not a property of the approximation scheme. However, the approximate data in figure 7 gives a proper qualitative view of final mass ratio and minimum a_o, which can be attributed to the approximation method.

It must nevertheless be acknowledged that the approximate solution is rather crude for this application.

Sources of Equivalent Length for Trajectory Problems

To improve the utility of the rest-to-rest problem model, L should be evaluated for each trajectory problem from a low-thrust type of solution that is close to the area of interest in terms of mode of rocket operation and acceleration level. But, as mentioned earilier, optimum low-thrust solutions are generally fraught with calculation difficulties.

The infinite-thrust or impulsive solution is currently the only available means of solving, with real speed and flexibility, point-to-point trajectory problems in the inverse-square gravity field. Unfortunately the equivalent L of impulsive solutions is apt to differ greatly from L evaluated at the low-thrust end of the acceleration scale. However, for very approximate but rapid estimates of low-thrust propellant requirements, L can be evaluated from the ΔV of impulsive transfers.

Two low-thrust types of optimum trajectory solution appear to minimize computation problems. These are the constant thrust all-propulsion and the power-limited variable thrust methods. Either method, however, requires numerical integration techniques and, therefore, a large investment in calculation time.

The all-propulsion case is the most simple constant thrust solution possible in the low-acceleration range, due to the elimination of coast phases in the numerical integration of the trajectory. Examples of L for constant thrust all propulsion were noted in figures 2 to 6.

The power-limited variable thrust, optimum solution method is described in references 3 and 4. This mode of rocket operation appears to be a great departure from the constant thrust mode. Acceleration and jet velocity are left free to vary along the optimum trajectory, constrained only by the requirement that the vehicle be power-limited, meaning that the product of thrust and jet velocity be constant. In this one respect, the constant thrust mode is also power-limited, since the product of thrust (constant) and jet velocity (constant) is also constant. Experience has shown that the variable thrust approach presents a somewhat simpler computation problem than the constant thrust all-propulsion method and provides values of equivalent length that compare favorably with constant thrust.

For the purpose of comparison with the constant thrust data given in figures 2 to 6, table I is given. In the variable thrust mode of rocket operation, propulsive requirement is given by J, the integral over the flight time of the square of the acceleration; that is,

$$J \equiv \int_0^T a^2 \, dt$$

A value of J can be found for each of the trajectories and used to evaluate an L, which is in agreement with the low acceleration end of the curves. The relation between J and L for rectilinear rest-to-rest variable thrust trajectories is developed in appendix B.

Figure 8 is given to illustrate an overall comparison between L evaluated from constant thrust all-propulsion, variable thrust, and impulsive trajectory solutions for Mars and Jupiter capture cases. Only the optimum heliocentric travel angle solution is recorded at each travel time for each mode of operation. Since the travel angle at which the propulsion requirement (J or ΔV) minimizes depends on the mode of rocket operation, figure 8 does not compare identical point-to-point transfer problems.

The difference between the impulsive and constant thrust optimum travel angle is greatest at the Hohmann (minimum energy) travel times - 260 days for Mars and 1000 days for Jupiter. The angular difference is only about 10 degrees for Mars but is about 100 degrees in the Jupiter example. In both cases, impulsive data is not shown beyond the Hohmann time since the requirements for optimum impulsive transfers in this region are involved and beyond the scope of this report.

Differences in optimum travel angle at each time are much smaller when variable thrust and constant thrust results are compared. For the Mars capture the angular difference is insignificant throughout the range shown. In the Jupiter case, the difference is more noticeable, growing steadily with T to about 30 degrees (out of 300 degrees) at 1000 days.

For the impulsive thrust results L is evaluated from equation (7) and ΔV. The variable thrust results show L evaluated from J and equation (B8) at each travel time. The third curve on each figure shows L evaluated from optimum constant thrust all-propulsion solutions using equation (20).

Figure 9 is given to aid in the comparison of the data shown in figure 8(a). By using the constant thrust all-propulsion value of L at each travel time as a base, an error criterion $\mathcal{E}$ may be defined

$$\mathcal{E} = \frac{L' - L_{ctm}}{L_{ctm}}$$

where L_{ctm} is the constant thrust value of L and L' is the value of L obtained from some other mode of operation. It can be seen in figure 9 that the variable thrust data provides the most consistent representative value of L throughout the range. However, the impulsive thrust data may be deemed quite acceptable for many trajectory analysis applications, taking into consideration the relatively high speed at which impulsive solutions may be obtained.

As an aid to the reader in further comparisons or performance calculations, equivalent length curves are given in appendix D for other interplanetary capture trajectories. The data in this appendix are derived from actual optimum solutions employing the constant thrust all-propulsion mode of operation. As in figure 8, the data in appendix D is limited to the optimum heliocentric travel angle at each transfer time.

Examples

Thus far, the approximate method has been discussed from the standpoint of comparisons of equivalent L and the effect of error in L. The aim of the following sections is to present more specific examples of the use of the approximation in generating ΔV and propellant requirement.

A comparison of approximate ΔV with exact trajectory calculation results is given in figure 10. In figure 10(a), the impulsive solution is used as a reference and in figure 10(b), the variable thrust solution is used.

In figure 10 the trajectory problem in question is a heliocentric capture trajectory from Earth to Mars. With specific impulse fixed at 6000 seconds, one curve on each figure shows ΔV against a_0 for optimum constant thrust solutions with coasting. The coasting solution curve joins with another, more horizontal, curve consisting of all-propulsion solutions along which specific impulse varies from 1000 seconds to infinity. The equivalent ΔV of the actual solutions, evaluated with equation (6) using the jet velocity and exact propellant fractions, is shown for a wide range of a_0 from less than 10^{-3} meters per second squared to infinity.

The approximate curves shown here faithfully follow the characteristics of the exact solutions. All the approximate values of ΔV shown are calculated using equations (18), (6), and one reference value of L obtained from the impulsive solution of the problem (in fig. 10(a)) or the variable thrust solution (in fig. 10(b)).

For figure 10(a), an accurate impulsive solution of the Mars capture trajectory is calculated in the inverse-square gravity field and found to require a total ΔV of 10 961 meters per second. Then, equation (7) is used to evaluate an equivalent length L in the field-free rectilinear model that corresponds to the given ΔV and transit time T of 140 days. Therefore,

$$L = \frac{T}{2} \Delta V = 0.66292 \times 10^{11} \text{ m}$$

The inverse-square field Mars capture problem is thereby transformed into an equivalent rectilinear rest-to-rest problem consisting of a 140-day transit time and a distance

to be travelled of 0.66292×10^{11} meters. For each desired a_o and v_j equation (18) is solved for the required propulsion time to satisfy L and T. Then, equation (6) is used to evaluate the ΔV from each value of the quantity $(1 - a_o t_p/v_j)$.

A slightly different procedure is used to describe the all-propulsion portion of the curve. For all-propulsion solutions, the propulsion time must equal the transit time, 140 days. The parameters a_o and v_j are no longer completely independent but are tied together by the stipulation that $t_p = T$ and that L and T are defined. For each value of v_j, equation (21) is used to calculate the necessary value of a_o for an all-propulsion solution. Thus,

$$a_o = \frac{4L}{T^2}\left(\frac{v_j}{v_j + \frac{L}{T}}\right)^2 \tag{21}$$

Then, as before, equation (6) yields a value of ΔV for each value of the quantity $(1 - a_o T/v_j)$.

The procedure for calculating the approximate data in figure 10(b) is identical to the method given for figure 10(a). The only exception occurs in the first step, which is the evaluation of the equivalent length L.

In figure 10(b), the reference solution of the trajectory problem is the variable thrust method described in references 3 and 4. For the 140-day 103-degree Mars capture trajectory, the variable thrust propulsive requirement J is obtained from precalculated data

$$J = 33.11\ m^2/sec^3$$

where

$$J \equiv \int_0^T a^2\, dt$$

The equivalent length of a variable thrust rectilinear flight can then be evaluated for the 140-day trip time by using equation (B8)

$$L = \sqrt{\frac{JT^3}{12}} = 0.6988\times10^{11}\ m$$

It is noted that the L obtained from the varible thrust reference case is higher than

the impulsive reference value. The approximate data in figure 10(b) appears more accurate than the approximate data in figure 10(a) except at high values of a_o.

For the final part of this section, a comparison of actual and predicted mass performance will be made, in figure 11, for constant thrust solutions of a Mars capture trajectory problem over a wide range of a_o and v_j.

In figure 11, the final mass ratio m_f/m_o is shown as a function of initial acceleration a_o along lines of constant specific impulse I. The "exact" data in the figure are obtained by repeated, numerically integrated, constant thrust mode optimum solutions of the Earth to Mars transfer at various combinations of I and a_o. Circular, coplanar heliocentric orbits are specified at each end of the trajectory, and net heliocentric transfer time and elapsed central angle are fixed. Hence, figure 11 is a family of constant thrust solutions of a given point-to-point trajectory problem in the inverse-square gravity field.

Final mass ratio decreases with decreasing a_o along each line of constant I. This variation of m_f/m_o is a reflection of the increasing ΔV discussed in sketch (a) and other figures. The lowest value of m_f/m_o for each I corresponds to all-propulsion solutions which, taken together, comprise the boundary curve labeled "all propulsion".

The dashed curves in figure 11 are approximate data obtained by using the method of this report. However, instead of manipulating the constant thrust rectilinear equations (eqs. (18) and (19)), the data in figure 11 are taken directly from the nondimensional curves given in appendix C. The curves in appendix C are precalculated, generalized solutions of constant thrust rectilinear rest-to-rest flight. Their use greatly simplifies hand calculations. The necessary steps are outlined in appendix C. Here again, only one reference solution of the given problem is required to evaluate a value of L, which is then assumed to hold constant for all values of a_o and I. The reference case used here was a power-limited variable thrust calculus of variations solution which, for the given problem, resulted in

$$J = \int_0^T a^2 \, dt = 6.03 \ m^3/sec^2$$

Equation (B8) is used to find the reference value of L for this trajectory problem based upon the given value of J

$$L = \sqrt{\frac{JT^3}{12}} = 6.27 \times 10^{10} \ m$$

Since the approximate data of figure 11 are based on the assumption that L is invariant, it is clear that, on the high-acceleration end of the figure, the value of L is

higher than need be, giving rise to poorer mass performance than the actual constant thrust solutions.

On the other hand, at the low-acceleration end of the scale, the reference value of L is not large enough. This is illustrated by the better than actual mass performance predicted by the approximate method and the relative shift of the approximate all-propulsion boundary to lower values of a_o. These observations are further demonstrations of the fact that the actual equivalent L of variational, constant thrust solutions varies with both a_o and the jet velocity.

Alternatively, another complete comparison plot could be generated for any other reference value of L. For example, a very high thrust (impulsive) solution of the same given point-to-point trajectory problem results in

$$\Delta V_{tot} = 5910 \text{ m/sec}$$

If equation (7) is used, this impulsive solution gives rise to a different reference value of L:

$$L = \frac{T \Delta V_{tot}}{2} = 5.87 \times 10^{11} \text{ m}$$

which differs from the variable thrust value by about 7 percent.

At very high a_o, the lower value of L from the impulsive solution would be in perfect agreement with the m_f/m_o of the actual data. But, the errors in m_f/m_o at the all-propulsion end of the curves would be further magnified.

Extended Problem Model

The primary aim of this report has been to analyze and apply a simple, rectilinear, rest-to-rest problem model to actual trajectory solutions. It has been found that in some areas this approach fails to correspond with actual flights to a degree sufficient for accurate approximation. The purpose of this section is to provide more background material on the nature of this problem by looking at the characteristic velocity profiles of actual trajectory solutions.

When the equivalent, field-free rectilinear velocity of actual constant thrust trajectory solutions in the inverse-square field are plotted with time, the result is often similar to sketch (e) (thrust is assumed to reverse at the end of the coast phase). The shape of the sketch indicates a departure from the rest-to-rest velocity profile.

The equivalent velocity given in equation (6)

$$\Delta V = -v_j \ln\left(1 - \frac{a_o t_p}{v_j}\right)$$

is evaluated at each instant of time along the flight as t_p increases. The actual amount of time spent in each propulsion period or coast period is taken from the optimum solution in the inverse-square field. In other words the rocket is operated on the straight-line path in field-free space using the same sequence of events given by the optimum solution of the inverse-square field trajectory problem.

Figure 12 is given to present more detail concerning the situation presented in sketch (e). Figure 12(a) is for the Jupiter capture heliocentric trajectory problem discussed in figure 4. The impulsive solution ($a_o = \infty$) is shown to consist of two velocity changes that are not equal in magnitude. The rectilinear velocity after the second ΔV (at $t = 400$ days) has been arbitrarily chosen as zero for a reference.

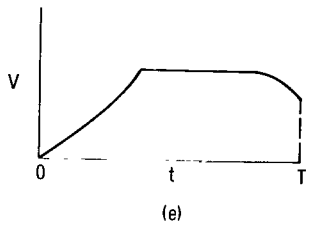

(e)

The two other velocity histories in figure 12(a) are given to show the effect of using low accelerations. Even in the low-acceleration cases, the difference between ΔV of each propulsion phase in close agreement with the difference present in the impulsive solution. The rectilinear distance covered (area under the velocity curves) is almost the same for all a_o. Clearly, this example shows that the actual optimum trajectory is similar in form to the rest-to-rest rectilinear problem model since the difference between the values of ΔV for each propulsion phase is small when compared to the total ΔV. Earlier, in figure 4, it was shown that the rest-to-rest values of L for this problem did not vary greatly with a_o.

The second part of the figure 12(b) is for the flyby trajectory problem to Mars. This case is an example of a wide discrepancy between the actual velocity profile of optimum trajectory solutions and the simple rest-to-rest rectilinear problem model. As indicated in figure 5, these dissimilarities can introduce significant error into the approximate scheme.

For this particular flyby problem, a point-to-point trajectory problem is specified such that the rocket encounters Mars' orbit after a given elapsed time and heliocentric central angle. Velocity and path angle are specified at both the initial and final points. The initial velocity and path angle correspond to circular orbit about the Sun at 1 A. U., but at Mars encounter the velocity and path angle are fixed at those values obtained from the impulsive flyby solution. (The same velocity and path angle were used as boundary conditions regardless of other acceleration levels used to allow the trajectory problem to be interpreted as a point-to-point problem.) The impulsive flyby trajectory solution in

the inverse-square field requires a ΔV at the start of the transfer but has no ΔV applied upon arrival at the planet encounter. For this example, the impulsive solution trajectory had an encounter velocity of 23 234 meters per second at an angle of 16.7 degrees relative to Mars' orbit path at encounter. This example would be more aptly termed a "limited flyby" because slightly different, but more optimum, values of terminal velocity and path angle could be found for each a_o in the inverse-square field problem.

In this flyby case, the initial value of characteristic velocity is arbitrarily taken to be zero. The optimal policy for the impulsive solution of this particular flyby problem is, as shown in the figure, to delay the application of the ΔV for about 35 days. The vehicle then coasts approximately 150 days, crossing Mars' orbit at the stated value of path angle and velocity on the 185th day. When the optimal solution is made with the low a_o of 1.4×10^{-3} meter per second squared, an initial delay period is still present in the solution (in this case, about 16 days) followed by a propulsion period of about 34 days. During this propulsion period, a ΔV only slightly greater than the impulsive value is applied. At the end of the transfer, a small propulsion period of about 4 days occurs just before arrival at the desired boundary conditions. The other low a_o case (0.5×10^{-3} m/sec^2) shows no initial delay period. The propulsion phase starts at $t = 0$ and continues on to a ΔV significantly higher than the impulsive ΔV. A terminal propulsion period is present again during which the equivalent rectilinear velocity is reduced to a value in close agreement with the other solutions. Again, as in the Jupiter example, the actual area under the velocity curves is nearly the same for all values of a_o and the difference between velocity increments in the propulsion phases is a consistent quantity. However, as can be seen, the velocity profiles indicate a significant departure from the simple rest-to-rest rectilinear problem model. Therefore, the rest-to-rest value of L varies as was shown in figure 5.

The facts presented in figure 12 strongly suggest that a more general type of rectilinear flight, with nonzero and unequal values of velocity at the boundaries, would be a better problem model for optimum trajectory solutions in the inverse-square gravity field. The use of this extended problem model has been briefly studied and appears to provide a markedly improved approximation method. However, it is not reported herein because it introduces much more complexity than the rest-to-rest problem model and the necessary detailed studies are not yet complete.

It is possible that the added complexity of the general model could outweigh the increased accuracy, making it undesirable in an approximation scheme. On the other hand, the rest-to-rest problem model is simple to analyze and use. Therefore, the rest-to-rest rectilinear model has been applied to cases such as the Mars flyby to demonstrate the error that may be introduced in approximating such trajectories with the over-simplified problem model.

CONCLUSIONS

It has been shown that the approximate evaluation of propulsive requirement for actual constant thrust trajectories can benefit greatly by the use of L, the equivalent straight-line distance traveled in gravity-free space. Length L is used in an analogous manner to the familiar ΔV of high-thrust trajectory analysis. In most cases, it provides a more consistent figure of merit among optimum trajectory solutions employing high- and low-thrust modes of rocket operation.

As interpreted by the methods of this report, equivalent L does vary slightly (6 to 10 percent) for a given trajectory problem, depending upon problem type and/or the acceleration level used. In some cases, the degree of variance of L may be great enough to cause too much inaccuracy in the evaluated propulsive requirement, but this depends upon the needs of the investigator. When the characteristic velocity profile of the actual flight trajectory departs radically from the rest-to-rest rectilinear model, as in the case of the flyby probes, the errors can be large. Due to the effect of I, typical low-thrust solutions show errors in m_f/m_o that are lower than errors in L by a factor of two or more.

The approximate results can be improved in comparison with numerically integrated results if the equivalent length of a trajectory problem is evaluated from the propulsive requirement of a low-thrust type of solution rather than an impulsive solution. In other words, if L is evaluated with one of the more easily calculated low-thrust methods such as variable thrust, or constant thrust, all-propulsion, it can give more accurate propulsive requirements for any other low-thrust solutions of the same problem. This entails much more calculation time than the impulsive thrust reference case approach. However, this alternative is still more economical than repeated numerical integration solutions of the same trajectory problem for each change in thrust level or jet velocity in the constant thrust mode of rocket operation, since only one exact, integrated reference case is needed for each trajectory problem.

At this writing, it is not certain that the rest-to-rest rectilinear trajectory provides the best problem model to use as a source of correlating equations for actual rocket flight. Although the present model is very simple to understand and apply, a more complicated problem model could introduce better correspondence with actual solutions and therby improve accuracy.

Lewis Research Center,
National Aeronautics and Space Administration,
Cleveland, Ohio, January 31, 1966.

APPENDIX A

SYMBOLS

a	acceleration, m/sec^2
F	thrust, N
g	standard gravity, 9.80665 m/sec^2
I	specific impulse, sec
J	$a^2\,dt$, m^2/sec^3
L	length, m
m	mass, kg
$\dot{m}$	magnitude of mass flow rate, kg/sec
P	power, W
r	final to initial mass ratio, m_f/m_o
T	transfer time, sec
t	time, sec
t_a	accumulated propulsion time, sec
t_p	total propulsion time, sec
V	velocity, m/sec
ΔV	characteristic velocity increment, m/sec
v_j	jet velocity, m/sec
$\dot{w}$	magnitude of weight flow rate
β	dimensionless initial acceleration, $L/a_o T^2$
γ	dimensionless jet velocity, $L/v_j T$
δ	dimensionless velocity increment, $T\,\Delta V/2L$
τ	dimensionless propulsion time, t_p/T
φ	heliocentric travel angle, deg

Subscripts:

f	final
max	maximum
min	minimum
o	initial
p	propellant
tot	total

APPENDIX B

RECTILINEAR REST-TO-REST SOLUTIONS

Constant Acceleration

Flight with constant acceleration is simply a special case of constant thrust. In this case, jet power is ignored, thrust is assumed constant, and the mass flow rate is assumed zero. A rest-to-rest rectilinear flight with constant acceleration is shown in sketch (f).

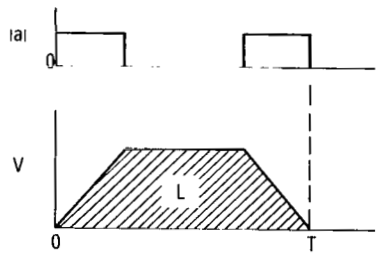

(f)

Since the acceleration is constant, dV/dt is the same in in each propulsion phase, except for a change in algebraic sign. If t_p is the total propulsion time, then each propulsion phase time is $t_p/2$ and the velocity at the coast phase is $at_p/2$. By simple addition of areas in the velocity history, the length may be expressed as a function of a, t_p, and T

$$L = \frac{at_p}{4}(2T - t_p) \tag{B1}$$

The characteristic velocity increment ΔV for this case is given by the integral of the acceleration magnitude. For constant acceleration,

$$\Delta V = \int_0^{t_p} |a| \, dt = at_p$$

For a given L, T, and t_p, a is defined; therefore, ΔV could be written as

$$\Delta V = at_p = \frac{4L}{2T - t_p} \tag{B2}$$

The all-propulsion case for constant acceleration derives directly from equations (B1) and (B2) by simple substitution of T for t_p. Hence, for all-propulsion, constant acceleration,

$$L = \frac{aT^2}{4} \tag{B3}$$

and

$$\Delta V = aT$$

Or, for a given L and T, since $a = 4L/T^2$,

$$\Delta V = \frac{4L}{T} \tag{B4}$$

Variable Thrust

It is also possible to develop equations involving the characteristic length L for the mode of rocket operation often known as "variable thrust". In this case, the jet power of the rocket is assumed constant but the acceleration level is left free to follow the best course of action to minimize propulsive effort for a given trajectory problem. For a rectilinear flight in field-free space, the optimal acceleration history is a linear variation with time (ref. 4). In the case where initial and final velocities are stipulated as zero, such as shown in sketch (g), the magnitude of the initial and final accelerations are equal. The acceleration decreases linearly from its initial value to zero at time T/2. The acceleration would then be reversed and made to increase in magnitude until the final time T. The acceleration history for this case is given by

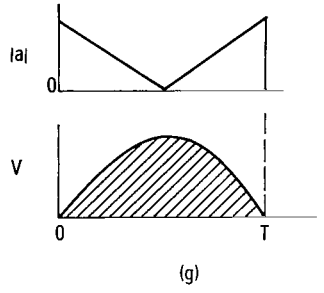

(g)

$$a = a_o \left(1 - \frac{2t}{T}\right) \tag{B5}$$

where a_o is the initial value, T is the total time, and t is any time between 0 and T. Integration of equation (B5) over the trip time results in the following equation for length L:

$$L = \frac{a_o T^2}{6} \tag{B6}$$

The usual figure of merit for propulsive effort in variable thrust trajectory analysis is J where

$$J \equiv \int_0^T a^2 \, dt$$

For any constant power electric rocket, whether constant thrust or variable thrust, the mass fraction can be shown to be a function of J and the specific power rating of the rocket P/m_o

$$\frac{m_f}{m_o} = \frac{1}{1 + \frac{J}{2\frac{P}{m_o}}}$$

In variable thrust analysis, the utility of J is enhanced by the fact that J is an invariant of each trajectory solution, regardless of the P/m_o used. In the constant thrust case, however, J is not as useful because it varies with the choice of a_o and v_j in solving a particular trajectory problem.

If the square of the acceleration in equation (B5) is integrated over the flight time, it is seen that for the rectilinear rest-to-rest problem J depends upon the initial acceleration a_o and travel time T. Then

$$J \equiv \int_0^T a^2 \, dt = \frac{a_o^2 T}{3} \tag{B7}$$

From equation (B6), length is a function of the a_o and time of travel. If equation (B7) is substituted into equation (B6), length is shown to depend upon J and travel time:

$$L = \sqrt{\frac{JT^3}{12}} \tag{B8}$$

APPENDIX C

GENERALIZED CONSTANT THRUST ROCKET PERFORMANCE

The equations developed in the main body of this report for the rectilinear flight of a constant thrust rocket may be generalized in terms of dimensionless parameters. This procedure makes possible the presentation of generalized performance charts for the constant thrust rocket, in terms of its operating parameters, which apply to any combination of travel length and travel time.

Constant Thrust With Coasting

Repetition of equation (18) shows how L, v_j, t_p, a_o, and T are interrelated

$$L = \frac{v_j^2}{a_o}\left(1 - \sqrt{1 - \frac{a_o t_p}{v_j}}\right)^2 - \frac{(T - t_p)}{2} v_j \ln\left(1 - \frac{a_o t_p}{v_j}\right) \qquad \text{(C1)}$$

Now let acceleration, jet velocity, and propulsion time be represented by the dimensionless parameters β, γ, and τ, respectively. Then,

$$\beta \equiv \frac{L}{a_o T^2} \qquad \beta > 0$$

$$\gamma \equiv \frac{L}{v_j T} \qquad \gamma > 0$$

$$\tau = \frac{t_p}{T} \qquad 0 < \tau < 1$$

Substitution of β, γ, and τ in the length equation in place of a_o, v_j, and t_p results in the cancellation of L and T, and equation (18) becomes

$$1 = \frac{\beta}{\gamma^2}\left(1 - \sqrt{1 - \frac{\gamma\tau}{\beta}}\right)^2 - \frac{(1 - \tau)}{2\gamma} \ln\left(1 - \frac{\gamma\tau}{\beta}\right) \qquad \text{(C2)}$$

It is noted here that the more familiar dimensionless quantities, propellant fraction and final mass fraction, can also be expressed in terms of β, γ, and τ; that is,

$$\frac{m_p}{m_o} = \frac{a_o t_p}{v_j} = \frac{\gamma\tau}{\beta}$$

and

$$\frac{m_f}{m_o} = 1 - \frac{m_p}{m_o} = 1 - \frac{\gamma\tau}{\beta}$$

The following expression for the equivalent ΔV of a constant thrust rocket is recalled:

$$\Delta V = -v_j \ln \frac{m_f}{m_o}$$

This ΔV is now made dimensionless by dividing it by $2L/T$, the ΔV of a rectilinear rest-to-rest impulsive thrust solution. At the same time, m_f/m_o is replaced by its equivalent, $(1 - \lambda\tau/\beta)$, so that

$$\delta \equiv \frac{\Delta V}{\frac{2L}{T}} = -\frac{1}{2\gamma} \ln \left(1 - \frac{\gamma\tau}{\beta}\right) \tag{C3}$$

From equation (C3) final mass fraction can be expressed in terms of δ and γ in the following form:

$$\frac{m_f}{m_o} = 1 - \frac{\gamma\tau}{\beta} = e^{-2\gamma\delta} \tag{C4}$$

The propulsion time fraction τ may be obtained from equation (C4)

$$\tau = \frac{\beta}{\gamma} \left(1 - e^{-2\gamma\delta}\right) \tag{C5}$$

If equations (C3), (C4), and (C5) are substituted into equation (C2), the result is a form that allows direct calculation of β from a choice of γ and δ. First,

$$1 = \frac{\beta}{\gamma^2}\left[\left(1 - e^{-\gamma\delta}\right)^2 - \gamma\delta\left(1 - e^{-2\gamma\delta}\right)\right] + \delta$$

Then, rearranging terms results in

$$\beta = \left(\frac{\delta - 1}{\delta^2}\right)\left[\frac{(\gamma\delta)^2}{\gamma\delta\left(1 - e^{-2\gamma\delta}\right) - \left(1 - e^{-\gamma\delta}\right)^2}\right] \tag{C6}$$

Choosing a γ and δ for a dimensionless rectilinear flight is analogous to choosing v_j and ΔV in the usual case. The dimensionless initial acceleration β can then be calculated from γ and δ. Subsequent calculations of other pertinent performance data can also be made, such as

$$\frac{m_f}{m_o} = e^{-2\gamma\delta}$$

and

$$\tau = \frac{\beta}{\gamma}\left(1 - \frac{m_f}{m_o}\right) = \frac{\beta}{\gamma}\left(1 - e^{-2\gamma\delta}\right)$$

Figure 13 is a chart of solutions of equation (C6). In figure 13, dimensionless ΔV is plotted against dimensionless a_o along lines of constant, dimensionless v_j. Also shown in figure 13 is the boundary of all-propulsion solutions, along which both γ and β are interdependent.

All Propulsion

In all-propulsion cases for the constant thrust rocket τ is unity. For $\tau = 1$, equation (C2) further simplifies to

$$\frac{\gamma^2}{\beta} = \left(1 - \sqrt{1 - \frac{\gamma}{\beta}}\right)^2 \qquad \text{(all propulsion)} \tag{C7}$$

Equation (C6) can be solved for either β or γ; thus,

$$\beta = \frac{(1+\gamma)^2}{4}\frac{\gamma)^2}{4} \qquad \text{(all propulsion)} \tag{C8}$$

and

$$\gamma = 2\sqrt{\beta} - 1 \qquad \text{(all propulsion)} \tag{C9}$$

Since the minimum value of γ is zero, it can be seen in equation (C8) that the minimum all-propulsion value of β is 1/4. Recalling that $\beta = L/a_o T^2$, it can be seen that the maximum a_o for all-propulsion cases occurs when β is minimum and is

$$a_o = \frac{L}{\beta T^2} = \frac{4L}{T^2} \qquad \text{(all propulsion and } \gamma = 0\text{)}$$

This maximum a_o occurs only for $\gamma = 0$, corresponding to infinite jet velocity.

For all-propulsion cases, equation (C3), the expression for dimensionless ΔV, is now rewritten for $\tau = 1$ so that

$$\delta = -\frac{1}{2\gamma} \ln\left(1 - \frac{\gamma}{\beta}\right)$$

Substituting for β in terms of γ from equation (C8) means that δ can be expressed in terms of γ

$$\delta = \frac{1}{\gamma} \ln\left(\frac{1+\gamma}{1-\gamma}\right) \qquad \text{(all propulsion)} \tag{C10}$$

Also, for $\tau = 1$, the final mass fraction becomes

$$\frac{m_f}{m_o} = 1 - \frac{\gamma}{\beta} \qquad \text{(all propulsion)}$$

Or, in terms of γ only,

$$\frac{m_f}{m_o} = \left(\frac{1-\gamma}{1+\gamma}\right)^2 \qquad \text{(all propulsion)} \qquad \text{(C11)}$$

The next figure, figure 14, is a generalized performance chart in which final mass fraction is plotted as a function of β along lines of constant γ. As in figure 13 the independent variables of figure 14 are the initial acceleration parameter β and the jet velocity parameter γ. However, at each β and γ pair, the δ of figure 13 has been converted into a value of m_f/m_o with the expression $m_f/m_o = e^{-2\gamma\delta}$.

Figure 14 then depicts the variation of final mass fraction with initial acceleration along lines of constant jet velocity. It can be directly converted into a data curve for any constant thrust trajectory problem once the equivalent length L and travel time T are defined. This procedure was used in the generation of the approximate data curves in figure 11.

The range of the initial acceleration parameter β, shown in figures 13 and 14, spans from the all-coasting impulsive case ($\beta = 0$) to the all-propulsion no-coasting case defined by the all-propulsion boundary curve. The propulsion time fraction τ varies between 0 and 1 along each γ curve. In many constant thrust trajectory problems, τ may be a more important parameter than β, since thrustor operating life may be more severely constrained than initial thrust to mass ratio of the electric vehicle. It is for this reason that figure 15 is presented.

In the final generalized chart given here (fig. 15) m_f/m_o is plotted against τ along lines of constant δ. The data is directly derived from figure 14 using the relation

$$\tau = \frac{\beta}{\gamma}\left(1 - \frac{m_f}{m_o}\right)$$

Figure 15 shows the steady decrease in final mass fraction between the impulsive ($\tau = 0$) and all-propulsion ($\tau = 1$) extremes of constant thrust operation.

An example of one use of these curves is given as figure 11. In this case, the data for m_f/m_o against a_o along lines of constant I is taken directly from figure 14. The dimensionless data in figure 14 is transformed into dimensioned data for figure 11 by simply applying the appropriate scale factors. These factors are functions of the transfer time T and the equivalent L of the trajectory in question. At each point in figure 11

$$a_o = \frac{1}{\beta}\frac{L}{T^2}$$

and

$$v_j = Ig = \frac{1}{\gamma}\frac{L}{T}$$

Hence, the approximate data curves shown in figure 11 are simply a dimensioned version of figure 14.

As an example of another use of these charts, consider the heliocentric flight of a 600-day capture probe to Jupiter. If the optimum travel angle case is used, the length can be read from figure 8(b) as 5.4×10^{11} meters. If ion thrustors with a jet velocity of 80 000 meters per second and an allowable propulsion time of 10 000 hours are assumed, the required a_o and m_f/m_o of the trajectory can be found in figures 14 and 15. First the value of γ is calculated with $T = 600$ days so that

$$\gamma = \frac{L}{v_j T} = \frac{5.4\times10^{11}}{(8\times10^4)(600)(86\ 400)} = 0.13$$

Then the propulsion time fraction is calculated, based on the allowable 10 000 hours

$$\tau = \frac{t_p}{T} = \frac{10^4}{(24)(600)} = 0.695$$

In figure 15 these values of γ and τ indicate that $m_f/m_o = 0.67$.

In figure 14, $\gamma = 0.13$ and $m_f/m_o = 0.67$ occur when $\beta = 0.275$. The required initial acceleration can then be calculated by the following equation:

$$a_o = \frac{F}{m_o} = \frac{L}{\beta T^2} = 0.73\times10^{-3}\ \text{m/sec}^2$$

APPENDIX D

EQUIVALENT LENGTH OF SOME SELECTED TRAJECTORY PROBLEMS

As mentioned in the main body, the purpose of this appendix is to present more equivalent length data for other interplanetary trajectories. The data curves shown here as figure 16 are based on numerically integrated, calculus of variations, interplanetary capture trajectories.

The particular mode of rocket operation used here is constant thrust, all propulsion. The specific impulse values used for each integrated solution are indicated on the respective curves. The value of I was set high to avoid severe mass changes.

Circular, coplanar heliocentric orbits are assumed for the Earth and other planets. Each trajectory begins with the vehicle in a circular orbit about the Sun at Earth's radius and ends with the vehicle again in circular orbit about the Sun at the target planet radius. The data given are somewhat limited in that only the optimum (minimum ΔV) heliocentric travel angle is used at each travel time. At each travel time, for each target planet, other heliocentric travel angles would be possible, although the propellant requirements would be greater and, hence, the equivalent length would be increased. Each trajectory solution was calculated to find the propellant fraction m_p/m_o and initial acceleration a_o required for the heliocentric, all-propulsion transit. Equation (20) was then used to evaluate the equivalent transit length L at each transit time T in the following manner:

$$L = \frac{v_j^2}{a_o}\left(1 - \sqrt{1 - \frac{a_o T}{v_j}}\right)^2 \qquad \text{(for all propulsion)}$$

where $v_j = I \times 9.80665$.

REFERENCES

1. Moeckel, W. E.: Trajectories with Constant Tangential Thrust in Central Gravitational Fields. NASA TR R-53, 1960.

2. Moeckel, W. E.: Fast Interplanetary Missions with Low-Thrust Propulsion Systems. NASA TR R-79, 1961.

3. Irving, J. H.; and Blum, E. K.: Comparative Performance of Ballistic and Low-Thrust Vehicles for Flight to Mars. Vol. II of Vistas in Astronautics, Morton Alperin and Hollingsworth F. Gregory, eds., Pergamon Press, 1959, pp. 191-218.

4. Melbourne, W. G.: Interplanetary Trajectories and Payload Capabilities of Advanced Propulsion Vehicles. Tech. Rept. 32-68, Jet Propulsion Laboratory, California Institute of Technology, Mar. 31, 1961.

5. Zimmerman, Arthur V.; MacKay, John S.; and Rossa, Leonard G.: Optimum Low-Acceleration Trajectories for Interplanetary Transfers. NASA TN D-1456, 1963.

6. Zola, Charles L.: Trajectory Methods in Mission Analysis for Low-Thrust Vehicles. Preprint No. 64-51, AIAA Jan. 1964.

7. Preston-Thomas, H.: A Note on "A Nuclear Electric Propulsion System." J. Brit. Interplanet. Soc., vol. 16, no. 9, Sept.-Oct., 1958, pp. 508-517.

TABLE I. - EQUIVALENT LENGTH GIVEN BY VARIABLE THRUST TRAJECTORY SOLUTIONS

Case	Transfer time, days	$J = \int a^2\,dt$, m^2/sec^3	Equivalent length, $L = \sqrt{JT^3/12}$, m
Mars capture	100	99.4	7.31×10^{10}
	140	33.1	6.99
	200	9.59	6.42
Mars flyby	185	2.65	3.0×10^{10}
Venus capture	140	6.92	3.20×10^{10}
Jupiter capture	400	85.3	5.42×10^{11}
0.1 AU solar probe	182.5	34.33	1.06×10^{11}

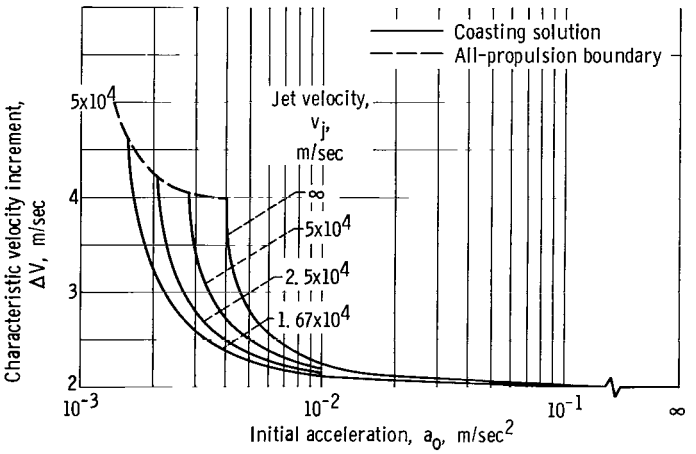

Figure 1. - Effect of initial acceleration and jet velocity on characteristic velocity increment for rectilinear rest-to-rest trajectory problem. Length, 10^{11} meters; transfer time, 10^7 seconds; constant thrust mode of operation.

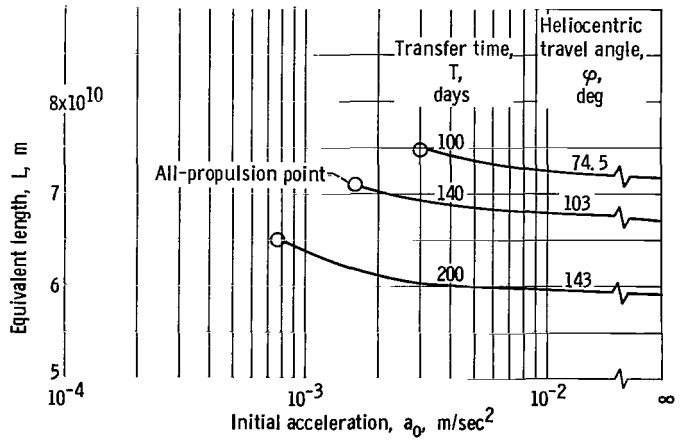

Figure 2. - Effect of initial acceleration on equivalent length for Earth-Mars capture trajectories at various transfer times and travel angles. Constant thrust mode; specific impulse, 6000 seconds.

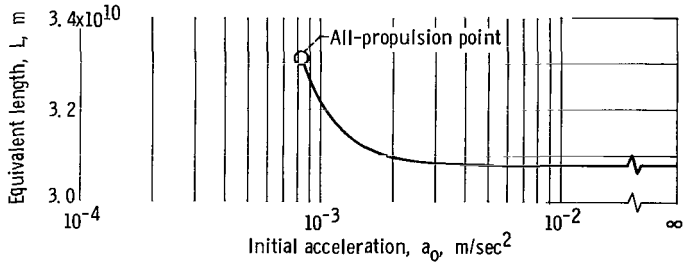

Figure 3. - Effect of initial acceleration on equivalent length for Earth-Venus capture trajectory. Transfer time, 140 days; heliocentric travel angle, 68.5 degrees; constant thrust mode; specific impulse, 6000 seconds.

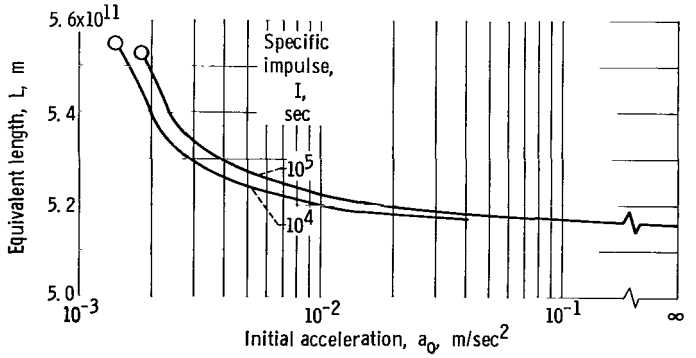

Figure 4. - Effect of initial acceleration and specific impulse on equivalent length for Earth-Jupiter capture trajectory. Transfer time, 400 days; heliocentric travel angle, 140 degrees; constant thrust mode.

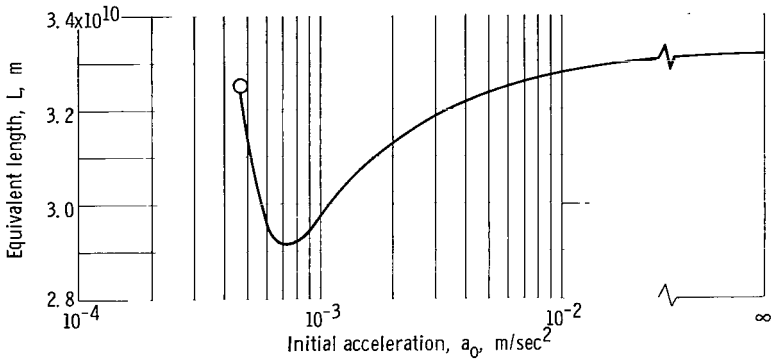

Figure 5. - Effect of initial acceleration on equivalent length for Earth-Mars flyby trajectory. Transfer time, 185 days; heliocentric travel angle, 154.5 degrees; constant thrust mode; specific impulse, 8000 seconds.

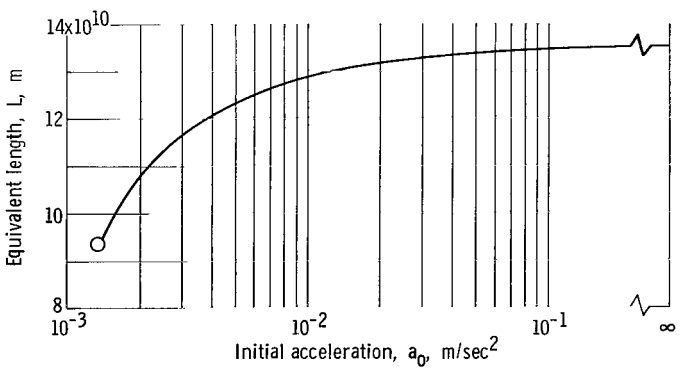

Figure 6. - Effect of initial acceleration on equivalent length for solar probe flyby to 0.1 A.U. Transfer time, 182.5 days; heliocentric travel angle, 265 degrees; constant thrust mode; specific impulse, 10 000 seconds.

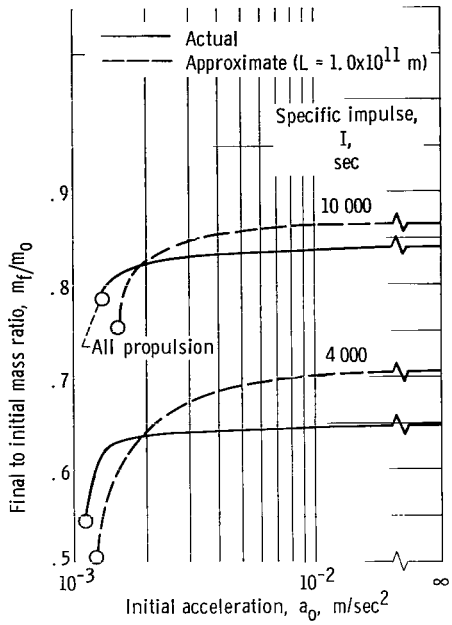

Figure 7. - Comparison of actual and approximate final to initial mass ratio for solar probe to 0.1 A. U. Transfer time, 182.5 days; heliocentric travel angle, 265 degrees.

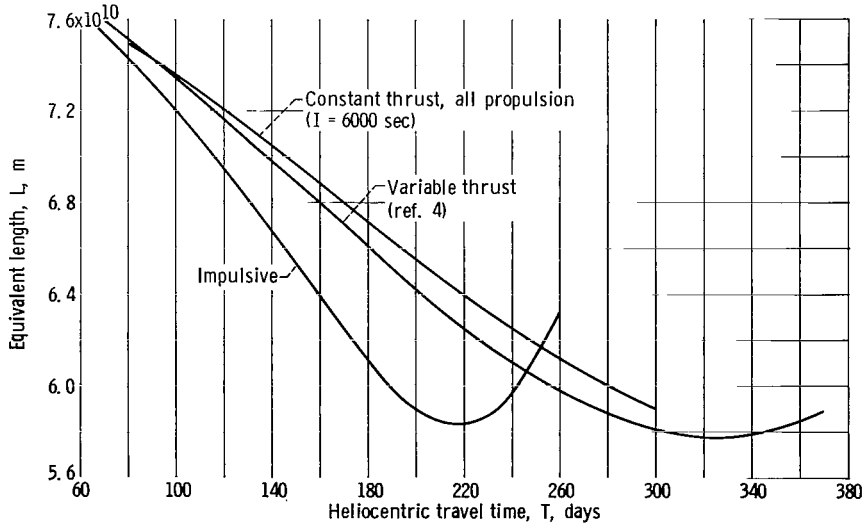

(a) Mars capture trajectories.

Figure 8. - Comparison of equivalent length from various sources based on actual propulsive requirement of trajectories with optimum travel angle at each travel time.

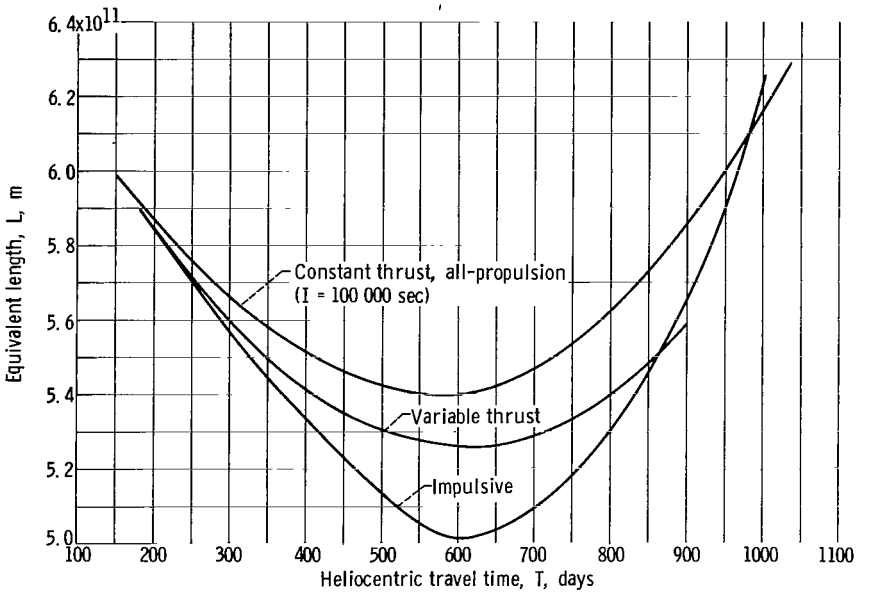

(b) Jupiter capture trajectories.

Figure 8. - Concluded.

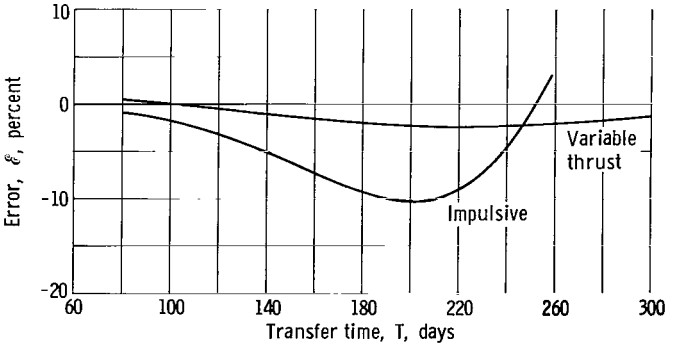

Figure 9. - Error comparison of equivalent lengths evaluated for Mars capture trajectories with optimum travel angle. Equivalent length of constant thrust all-propulsion solution used as reference.

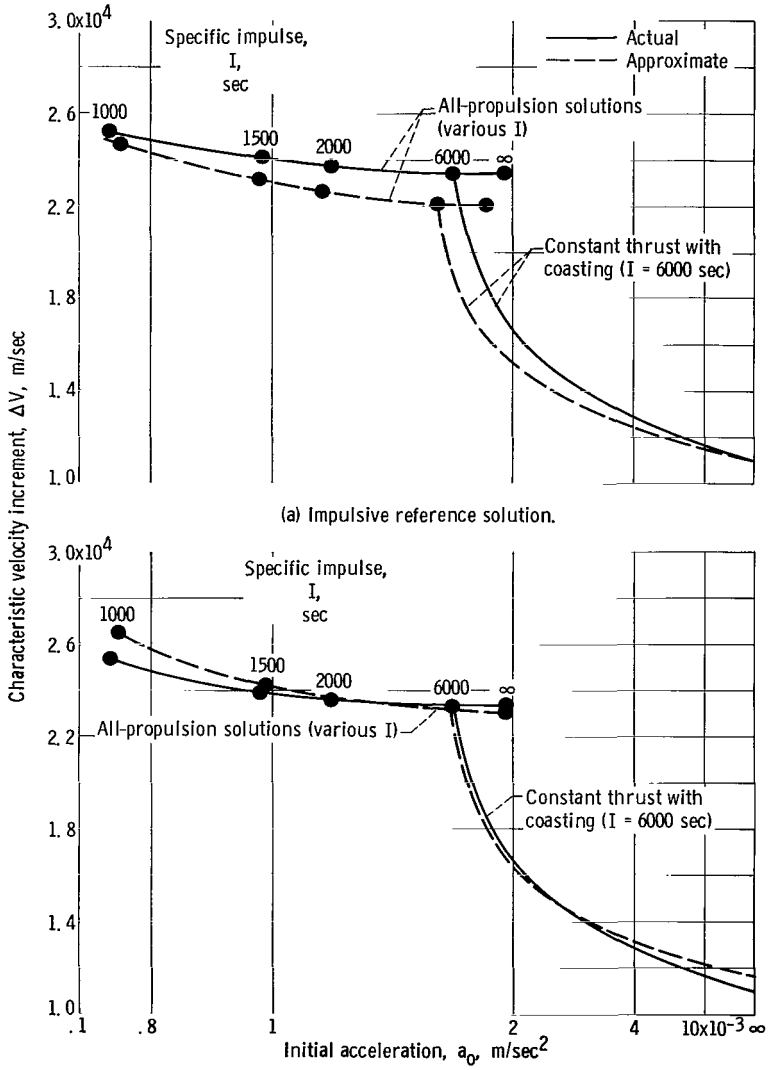

Figure 10. - Comparison of exact and approximate characteristic velocity increment for Earth-Mars capture trajectory. Transfer time, 140 days; heliocentric travel angle, 103 degrees.

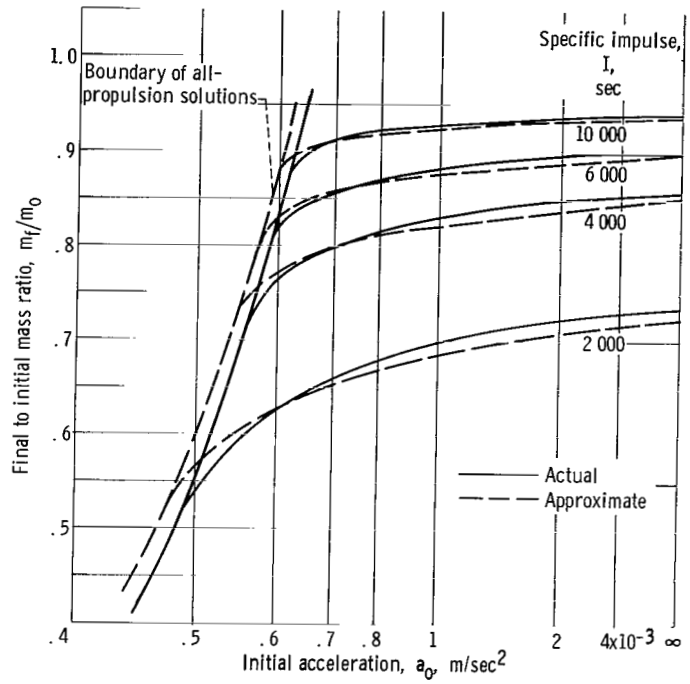

Figure 11. - Comparison of actual and approximate final to initial mass ratio for Earth-Mars capture trajectory. Transfer time, 230 days; heliocentric travel angle, 166 degrees. Constant thrust power-limited mode.

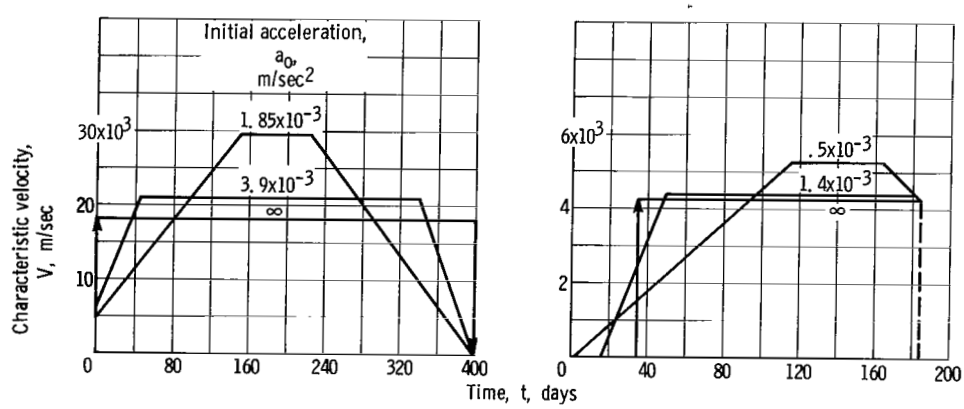

(a) For Jupiter capture trajectory. Transfer time, 400 days; heliocentric travel angle, 140 degrees; specific impulse, 100 000 seconds.

(b) For Mars flyby trajectory. Transfer time, 185 days; heliocentric travel angle, 155 degrees; specific impulse, 8000 seconds.

Figure 12. - History of characteristic velocity for optimum, constant thrust trajectory solutions in gravity field.

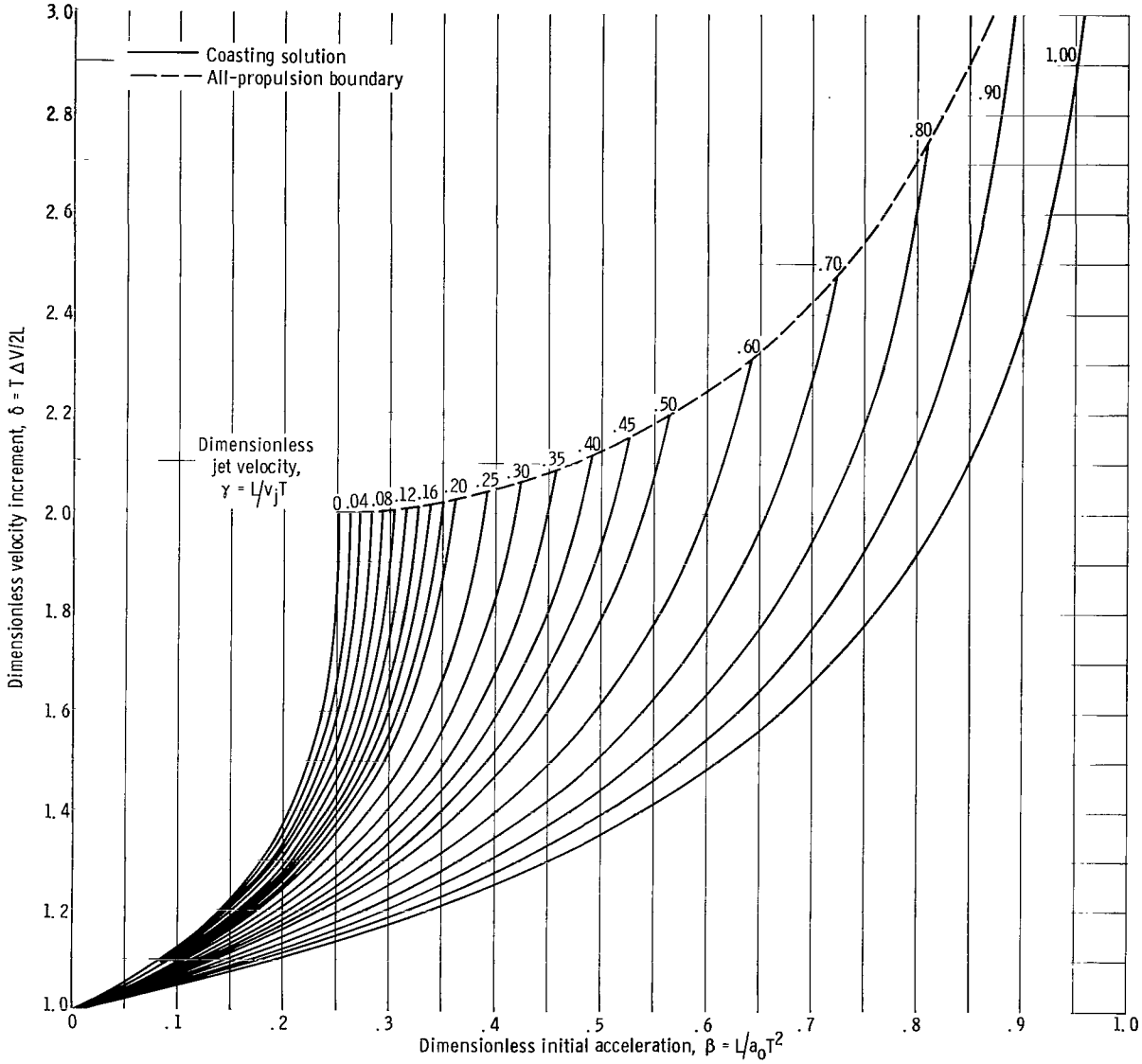

Figure 13. - Total velocity increment as function of initial acceleration and jet velocity (dimensionless ratios) for rectilinear rest-to-rest trajectories. Constant thrust mode.

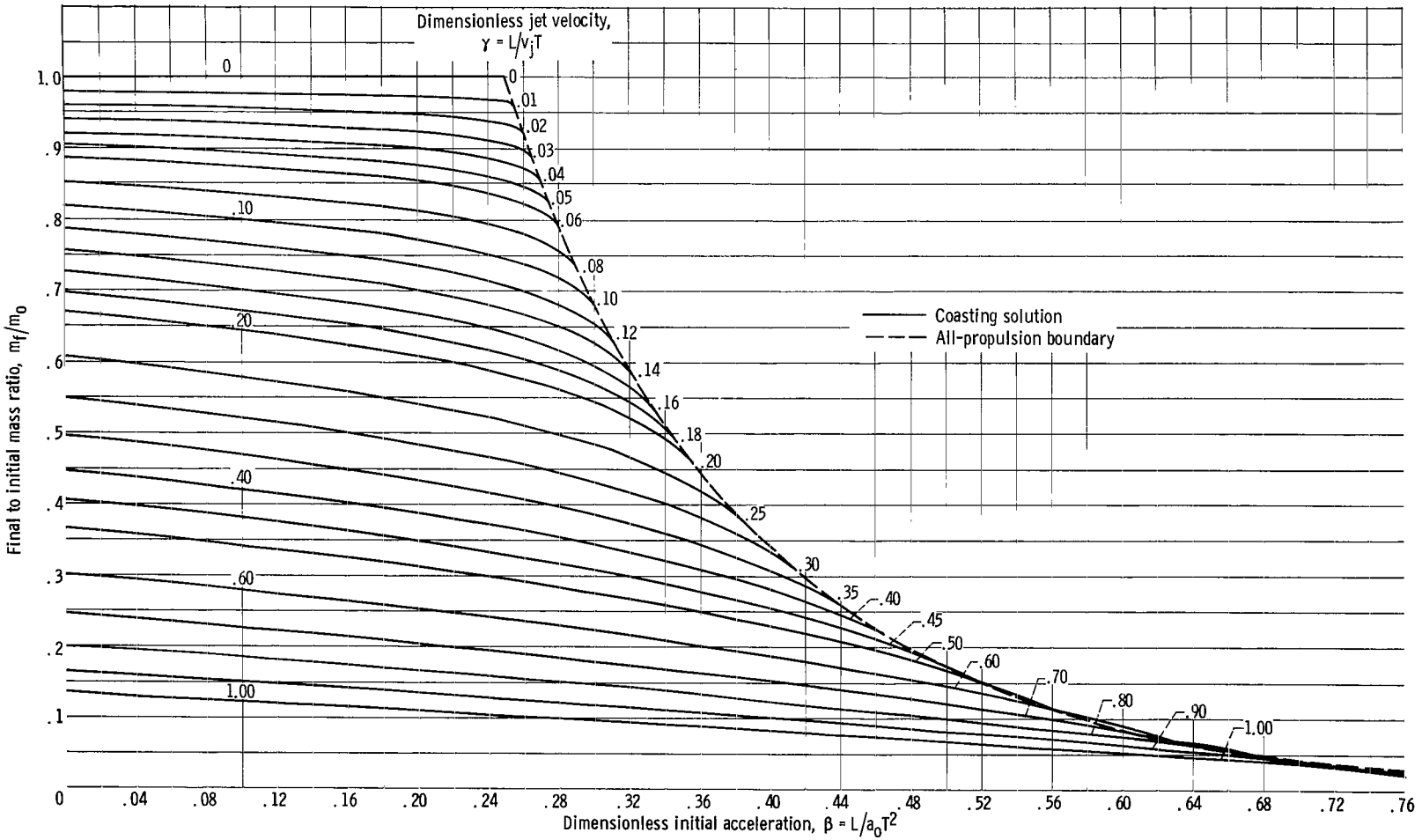

Figure 14. - Final to initial mass ratio as function of initial acceleration and jet velocity (dimensionless ratios) for rectilinear rest-to-rest trajectories. Constant thrust mode.

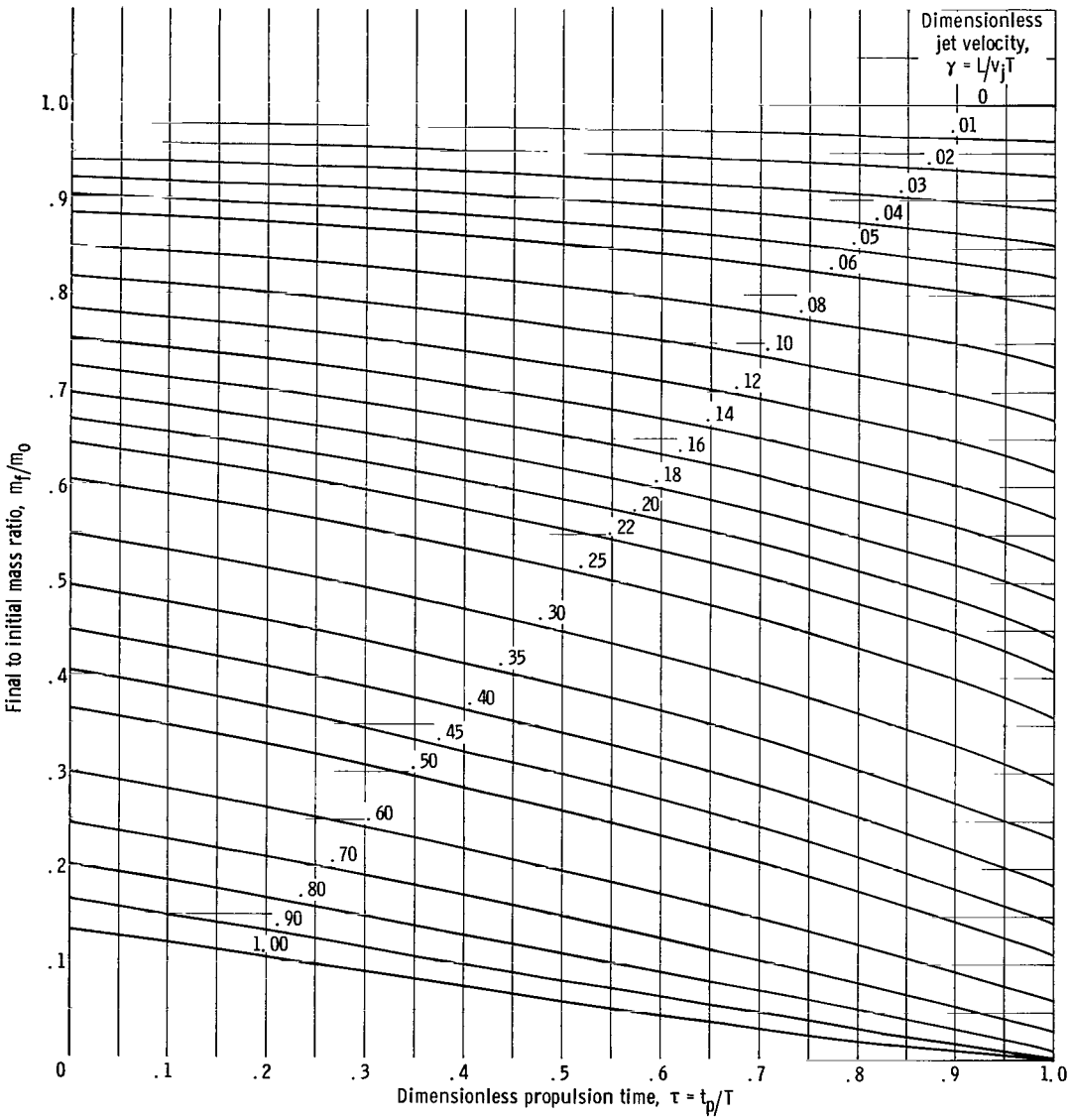

Figure 15. - Final to initial mass ratio as function of propulsion time and jet velocity (dimensionless ratios) for rectilinear rest-to-rest trajectories. Constant thrust mode.

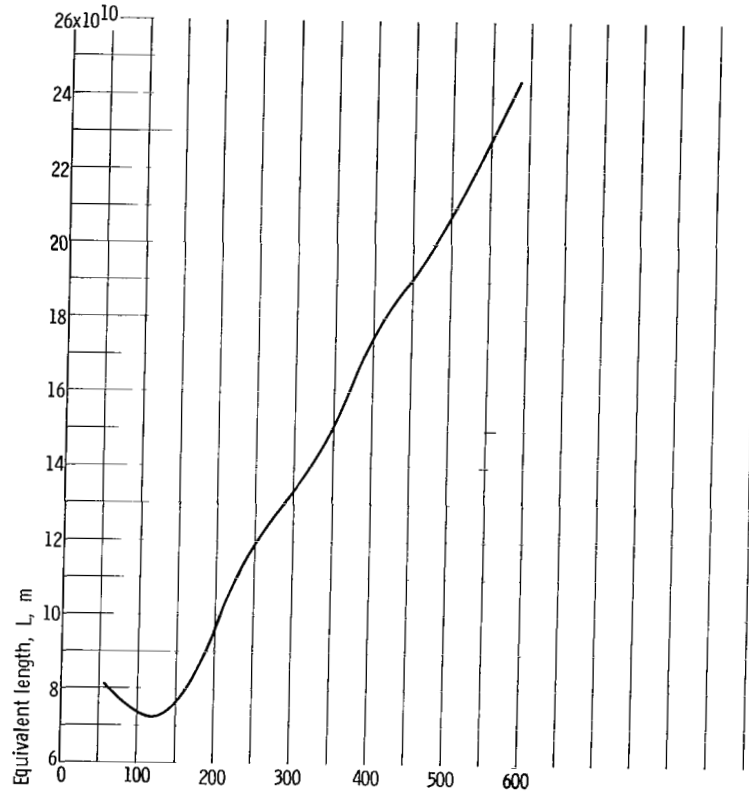

(a) Earth-Mercury capture trajectory. Specific impulse, 10 000 seconds.

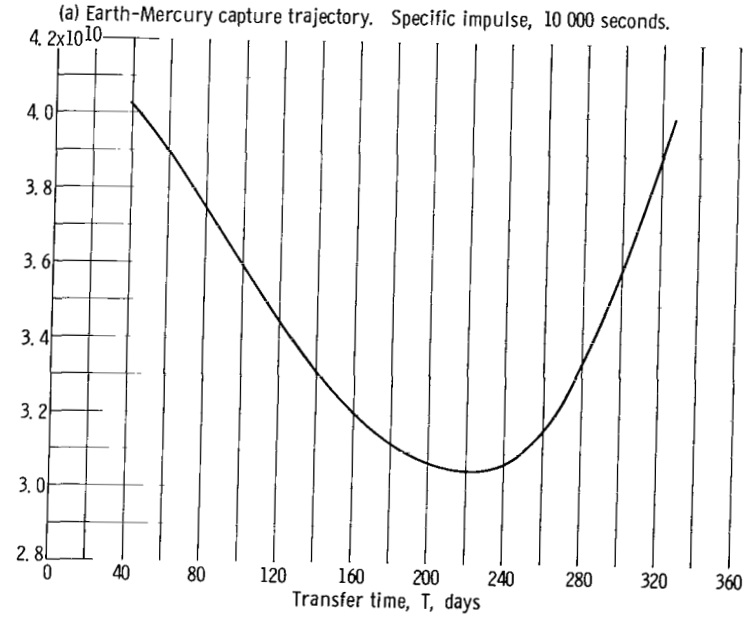

(b) Earth-Venus capture trajectory. Specific impulse, 10 000 seconds.

Figure 16. - Equivalent length curves for various interplanetary capture trajectories. Constant thrust all-propulsion mode.

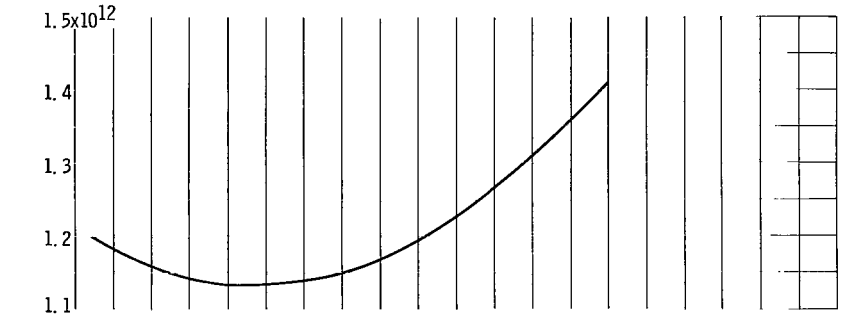

(c) Earth-Saturn capture trajectory. Specific impulse, 100 000 seconds.

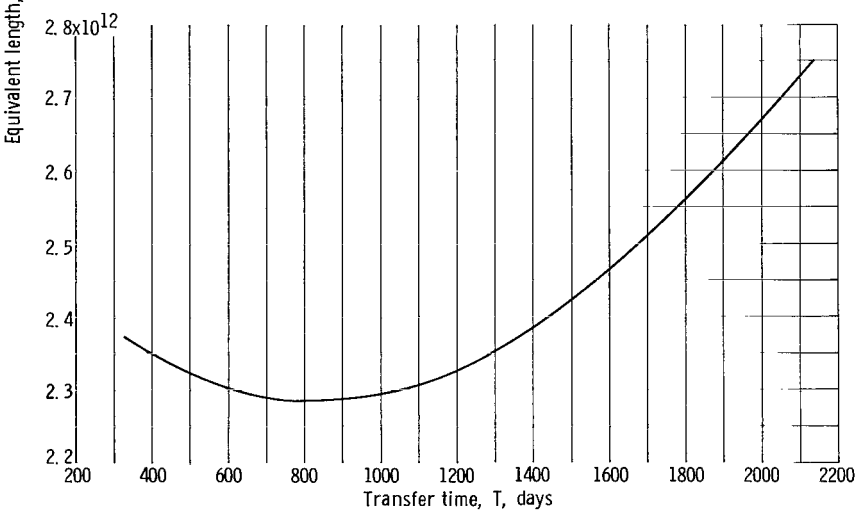

(d) Earth-Uranus capture trajectory. Specific impulse, 100 000 seconds.

Figure 16. - Continued.

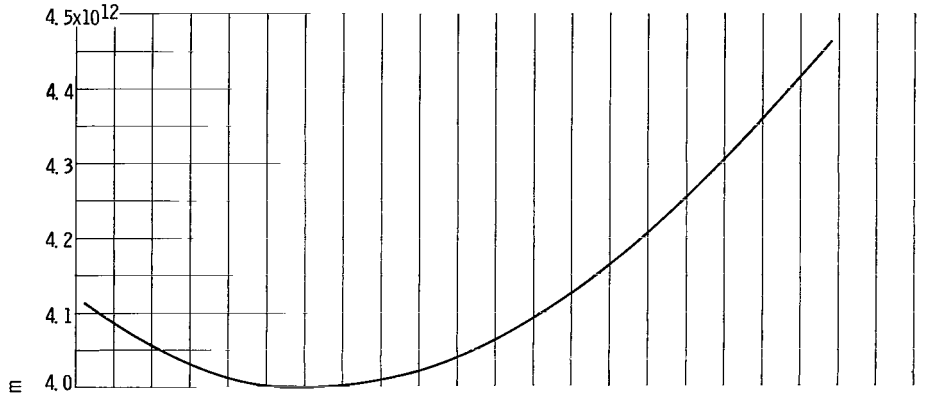

(e) Earth-Neptune capture trajectory. Specific impulse, 100 000 seconds.

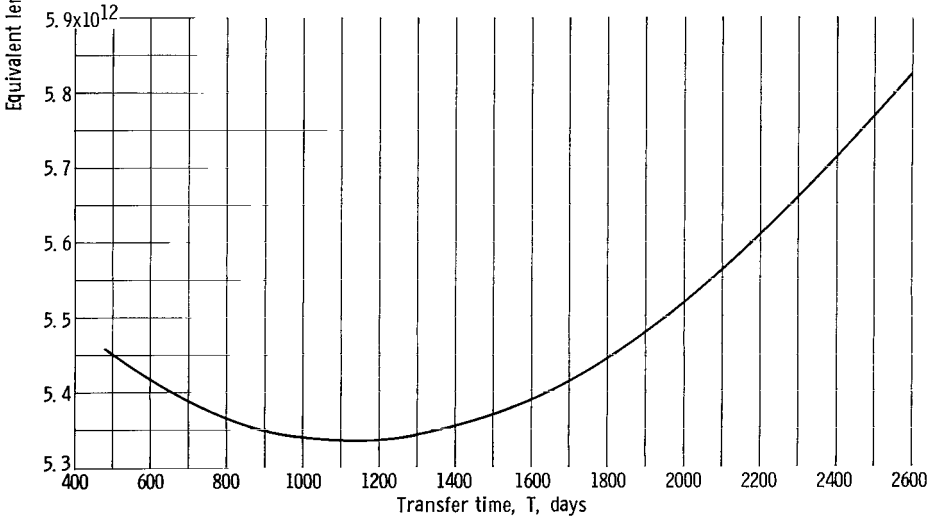

(f) Earth-Pluto capture trajectory. Specific impulse, 100 000 seconds.

Figure 16. - Concluded.

"The aeronautical and space activities of the United States shall be conducted so as to contribute . . . to the expansion of human knowledge of phenomena in the atmosphere and space. The Administration shall provide for the widest practicable and appropriate dissemination of information concerning its activities and the results thereof."

—NATIONAL AERONAUTICS AND SPACE ACT OF 1958

NASA SCIENTIFIC AND TECHNICAL PUBLICATIONS

TECHNICAL REPORTS: Scientific and technical information considered important, complete, and a lasting contribution to existing knowledge.

TECHNICAL NOTES: Information less broad in scope but nevertheless of importance as a contribution to existing knowledge.

TECHNICAL MEMORANDUMS: Information receiving limited distribution because of preliminary data, security classification, or other reasons.

CONTRACTOR REPORTS: Technical information generated in connection with a NASA contract or grant and released under NASA auspices.

TECHNICAL TRANSLATIONS: Information published in a foreign language considered to merit NASA distribution in English.

TECHNICAL REPRINTS: Information derived from NASA activities and initially published in the form of journal articles.

SPECIAL PUBLICATIONS: Information derived from or of value to NASA activities but not necessarily reporting the results of individual NASA-programmed scientific efforts. Publications include conference proceedings, monographs, data compilations, handbooks, sourcebooks, and special bibliographies.

Details on the availability of these publications may be obtained from:

SCIENTIFIC AND TECHNICAL INFORMATION DIVISION

NATIONAL AERONAUTICS AND SPACE ADMINISTRATION

Washington, D.C. 20546